Received: 10 December 2020 | Revised: 23 September 2021 | Accepted: 25 September 2021

DOI: 10.1002/jcla.24066

RESEARCH ARTICLE

WILEY

LncRNA MIR4435-2HG functions as a ceRNA against miR-125a-5p and promotes neuroglioma development by upregulating TAZ

Wangzhen Shen | **Jiawei Zhang** | **Yunfeng Pan** | **Yun Jin**

Department of Neurosurgery, Tongxiang First People's Hospital, Tongxiang, China

Correspondence
Yun Jin, Department of Neurosurgery, Tongxiang First People's Hospital, No. 1918, Jiaochang East Road, Zhendong New District, Tongxiang City, Zhejiang, China
Email: jinyunmr@163.com

Abstract

Background: Expression of the TAZ gene is closely related to the prognosis of glioma patients. We hoped to find long noncoding RNAs (lncRNAs) related to TAZ and a new target for glioma treatment.

Methods: TAZ-related genes were found by dual-luciferase reporter gene assay, and the correlation of each gene was analyzed by the Pearson method. Human glioma cell lines U87 MG and U251 and glioma rats were used for cytology assays, and the related genes were transfected. We conducted immunohistochemistry, RT-qPCR, Western blotting, CCK8 test, flow cytometry, transwell assays, clone formation analysis, and tumor weight measurements to verify the above relationship.

Results: We found that miR-125a-5p was closely related to the TAZ gene, and the lncRNA MIR4435-2HG was closely related to miR-125a-5p. Both MIR4435-2HG-OE and TAZ increased the expression of the TAZ gene, activated the Wnt signaling pathway, inhibited apoptosis, and promoted migration and proliferation in glioma cells. Besides, it also increased the tumor volume of gliomas in a rat model subcutaneously inoculated with glioma cells. We also found miR-125a-5p could block the effect of MIR4435-2HG-OE and TAZ.

Conclusions: LncRNA MIR4435-2HG obstructs the functions of miR-125a-5p and promotes neuroglioma development by upregulating the TAZ gene.

KEYWORDS
lncRNA MIR4435-2HG, miR-125a-5p, neuroglioma, TAZ, U251 cells, U87 MG cells

1 | INTRODUCTION

Glioma is the most common primary central nervous system tumor, accounting for more than half of all primary intracranial tumors.[1] According to the World Health Organization (WHO) classification scheme, gliomas can be divided into four types: mixed glioma, neuroepithelial tumor, gliomatosis cerebri, and neuroglioma.[2] The transcription coactivator TAZ, which contains 400 amino acids, is one of the most important downstream effectors of the mammalian Hippo pathway. Its structure consists of a transcriptional-enhanced associate domain (TEAD)-binding region (TB), a WW region, a curly helix structure, a transcription activation region, and a PDZ motif at the C-terminus.[3,4] TAZ is involved in the transcriptional co-activation of downstream target factors, and the regulation of cell proliferation, apoptosis, and migration.[5,6] In recent years, it has been found that the expression of TAZ in gastric cancer, non-small

cell lung cancer, breast cancer, and neuroblastoma is higher than in normal adjacent tissues.[7-10] This indicates that TAZ is an important target in malignant tumors. However, it is not clear how TAZ affects gliomas and what the related mechanism is. Through our research, we hoped to find the mechanism through which TAZ acts in gliomas.

At the same time, research this year has shown that long-chain noncoding RNAs can promote cell proliferation, eliminate cell growth inhibition, induce angiogenesis, and inhibit apoptosis.[11] Long noncoding RNAs (lncRNA) can regulate disease progression in multiple organs of the body in a variety of ways, including by affecting the corresponding signaling pathways and regulating microRNAs. Therefore, many lncRNAs can not only serve as indicators of disease diagnosis and prognosis, but can also be effective therapeutic targets.[12,13] Long-chain noncoding RNA plays an important role in tumor development.[14] In recent years, it has been reported that lncRNA MIR4435-2HG is highly expressed in hyper gliomas and may increase the expression of CD44 by adsorbing miR-125a-5p, thus affecting the signaling pathways of the epithelial-mesenchymal transition (EMT) and tumor necrosis factor-alpha (TNF-α).[15,16] These results suggested to us that the role of TAZ in gliomas might be related to long-chain noncoding RNA. Will the corresponding microRNAs be found? We collected human glioma samples and used bioinformatics to search for related genes, which were proven by cell-based assays.

2 | MATERIALS AND METHODS

2.1 | Brain tissue from patients with glioma, experimental cell culture, and cell transfection

In this study, immunohistochemical analyses were conducted on healthy brain tissues and brain tissues from glioma patients at our hospital between December 2017 and December 2018 to observe the expression of TAZ in the lesions of glioma patients. The study was divided into three groups: the control group with healthy brain tissue (15 cases), the experimental group with grade I–II glioma tissue and its para-carcinoma tissues (17 cases), and the experimental group with grade III–IV glioma tissue and its para-carcinoma tissues (23 cases). Healthy brain tissue was obtained from 15 patients with craniocerebral trauma who had no history of neurological changes. The grade of glioma was classified according to the WHO's histological classification of central nervous system tumors (2016).[17]

We used two cell lines: malignant glioma cell line U87 MG and malignant human glioma cell line U251. Both cell lines were cultured in Dulbecco's modified Eagle's medium (DMEM) (Invitrogen) supplemented with 10% fetal calf serum (HyClone) and 100 U/ml each penicillin and streptomycin (Gibco). The culture medium was changed every 48 h to ensure normal growth, and the cells were cultured at 37°C in a 5% CO_2 cell incubator. Both cell lines are adherent cells, and the cells used in the experiments were in the logarithmic growth stage.[18]

One day in advance, we inoculated 5×10^5 U87 MG cells/U251 cells in each well of a six-well plate. After 24 h of culture, the cells had adhered to the wall, and the fusion degree had reached about 60%. The cells were divided into six groups. A 2-ml aseptic Eppendorf (EP) tube was used to prepare the transfection liquid. Serum-free medium was added with OE-NC (negative control, treatment with lentivirus expressing irrelevant sequences), mimic NC (negative control), OE-NC + mimic NC, MIR4435-2HG-OE + mimic NC, OE-NC + miR-125a-5p mimic, MIR4435-2HG-OE + miR-125a-5p mimic, sh-NC (negative control), inhibitor NC (negative control), sh-NC + inhibitor NC, sh-MIR4435-2HG + inhibitor NC, sh-NC + miR-125a-5p inhibitor, or sh-MIR4435-2HG + miR-125a-5p inhibitor to tube A. OE-NC was the negative control for overexpression. Mimic NC was the miRNA analog and was also a negative control. Serum-free medium and lipofectamine™ 2000 liposomes were added to tube B. The solution in tube A was gently mixed with that in tube B and maintained at room temperature for 15 min. The cells were washed twice with medium, and then, the mixture from tubes A and B was poured onto the cells. The cells were cultured in a cell incubator at 37°C with 5% CO_2 for 24 h before the experiments were carried out.[19]

2.2 | Immunohistochemical analysis

The healthy brain tissue and glioma tissue were sectioned. The sections were successively immersed in xylene I (10 min), xylene II (10 min), anhydrous ethanol I (5 min), anhydrous ethanol II (5 min), 95% ethanol (5 min), 80% ethanol (5 min), and 70% ethanol (5 min) and then washed twice with deionized water for 2 min each time. Three percent hydrogen peroxide was added to the tissue sections to block endogenous peroxidase. The sections were incubated at room temperature for 15 min and then washed with PBS three times, each time for 3 min. PBS was removed with absorbent paper before 5% normal rabbit serum was added to the slide prior to sealing at 37°C for 30 min. The liquid around the tissue was dried with absorbent paper. The diluted primary antibody (anti-TAZ antibody, anti-rabbit, ab84927, Abcam) was added, and the sections were incubated overnight at 4°C in a wet box. The sections were washed three times with PBS, each time for 3 min. After the sections were dried with absorbent paper, HRP-labeled goat anti-human IgG (H+L) was added as the secondary antibody. The sections were incubated at 37°C for 30 min. The sections were then cleaned with PBS and dried with absorbent paper. DAB color solution was added to the section. The positive brown signal was observed under the microscope. Before the staining became too deep, the sections were washed under running water to stop the staining. Sections were dyed with Harris hematoxylin for 40 s. After washing with water, the sections were differentiated with 1% hydrochloric acid alcohol and then washed with tap water to return them to blue. The sections were dehydrated and fixed, and then successively put

into 70% alcohol, 80% alcohol, 90% alcohol, 95% alcohol, anhydrous ethanol I, anhydrous ethanol II, xylene I, and xylene II for dehydration, and transparency, and finally dried in the fume hood. Neutral gum was dropped beside the tissue on the slide. Sections were covered with a cover glass and dried. Images were recorded using a microscope.[20]

2.3 | Dual-luciferase reporter gene assay

The dual-luciferase reporter gene assay reagents (1× PLB lysate buffer, Luciferase Assay Reagent II (LAR II), Stop & Glo® Reagent) were prepared. Healthy brain tissue and glioma tissue were cut into pieces and ground. Then, 100–150 μl 1× lysate buffer PLB was added to them. The mixture was mixed on a shaking table for 30 min to ensure that the lysis buffer had completely lysed the cells. Using the dual-luciferase test (Promega GloMax), the system was reset (Tools-Settings-Reset). The dual-luciferase test program was set as follows: The detection system was set as tools, settings, and reset. The double luciferase detection procedure was set as protocols, run protocol, dlr-o-inj, and OK. The liquid in the EP tube was blown, mixed, and then was placed in the detector, and "measure" was clicked to start reading. Each sample had three values, RLU1—firefly luciferase reaction intensity, RLU2—internal reference sea kidney luciferase reaction intensity, and the ratio RLU1/RLU2, and the ratios were recorded.[21]

2.4 | Pearson test and analysis

SPSS 25.0 was used to analyze the data association. MIR4435-2HG, miR-125a-5p, and TAZ data were entered into SPSS 25.0 before clicking "analysis"—"correlation"—"bivariate" to select the variables. "Pearson" in the "correlation coefficient" box was selected. The data in this study were continuous variables. "Bootstrap" was selected to carry out the simulation analysis and get the Pearson correlation analysis result chart.[22]

2.5 | RT-qPCR

TRIzol (1 ml) was added to the transfected healthy brain tissue, glioma tissue, serum, U87 MG cells, and U251 cells, which were homogenized on ice, transferred to a new EP tube (1.5 ml), and incubated at room temperature for 5 min. Chloroform (0.2 ml) was added, and the mixture was oscillated (with strong shaking by hand) and maintained at room temperature for 5 min. The mixture was centrifuged at 4°C for 15 min at 6660 *g*. The upper water phase was transferred to a new EP tube, and 0.5 ml isopropanol was added. The tube was oscillated, mixed, and stored at room temperature for 10 min before centrifuging at 4°C for 15 min at 9590 *g*. The supernatant was poured out, and 1 ml 75% anhydrous ethanol was added (stored at 4°C). The mixture was oscillated and centrifuged at 4°C at 10,000 rpm for 5 min. The supernatant was removed and maintained at room temperature or 37°C for 20 min to dry the RNA precipitate. Then, 20 μl DEPC water were added to the EP tube. The RNA was fully dissolved after incubation at 60°C for 3–5 min (or held for 3–5 min). The RNA concentration was detected. Total RNA concentration = OD260 × 40 × dilution factor (150 times) μg/ml. Using reverse transcriptase, the resulting RNA was reverse transcribed into cDNA. Theprimerswereasfollows:TAZ:5′-ACCCACCCACGATGACCCCA-3′, 5′-GCACCCTAACCCCAGGCCAC-3′; miR-125-a-5p: 5′-GGTCATTCC CTGAGACCCTTTAAC-3′,5′-GTGCAGGGTCCGAGGT-3′.MIR4435-2 HG:5′-TGATAAAGGGCTCTGAAAGC-3′, 5′-CACGATGCCTTCACCA GTGT-3′. Polymerase chain reaction (PCR) was conducted, and a reaction system of 20 μl was adopted. The samples were run and analyzed using an Applied Biosystems real-time fluorescence quantitative PCR instrument.[23]

2.6 | Western blotting

We cultured U87 MG cells and U251 cells, divided them into six groups, and transfected them with OE-NC, mimic NC, OE-NC + mimic NC, MIR4435-2HG-OE + mimic NC, OE-NC + miR-125a-5p mimic, or MIR4435-2HG-OE + miR-125a-5p mimic. The transfected cells were disrupted with radio immunoprecipitation assay (RIPA) buffer. Total protein was extracted, and the protein was quantified by the bicinchoninic acid (BCA) method. Separate adhesives and concentrated adhesives were added to the electrophoretic splint before constant pressure electrophoresis at 80 V. For the transfer membrane, pure methanol was used to soak the PVDF membrane, and the transfer device was assembled as follows before tightening the splint: sponge → layer filter paper → glue → film → layer filter paper → sponge. The transfer tank was placed in an ice bath. It was then placed on the sandwich deck, transfer buffer was added, and the electrode was inserted and run at 250 mA for 2 h. After the membrane transfer, the membrane was placed in 25 ml 5% skim milk powder buffer solution for 1 h at room temperature. It was washed with 15 ml TBS/T three times (5 min each time). A primary antibody (TAZ (anti-TAZ antibody, anti-rabbit, ab84927, Abcam), β-catenin (anti-beta-catenin antibody, ab32572, Abcam), c-myc (anti-c-myc antibody, anti-rabbit, ab32072, Abcam), cyclin D1 (anti-cyclin D1 antibody, anti-rabbit, ab16663, Abcam), and β-actin (anti-actin antibody, anti-rabbit, ab179467, Abcam)) with appropriate dilution was added for incubation at room temperature for 1–2 h or 4°C overnight with slow shaking. The membrane was then washed with 15 ml TBS/T three times (5 min each time). Alkaline phosphatase (AP) or horseradish peroxidase (HRP)-labeled secondary antibody with appropriate dilution was added, and the membrane incubated at room temperature again for 1 h before washing with 15 ml TBS/T three times (5 min each time). It was washed with 15 ml TBS once. Finally, a gel imaging system was used for detection.[24]

2.7 | CCK8 assay for cell proliferation activity

We divided the cultured U87 MG and U251 cells into six groups and transfected with either OE-NC, mimic NC, OE-NC + mimic NC, MIR4435-2HG-OE + mimic NC, or MIR4435-2HG-OE + miR-125a-5p. The transfected U87 MG cells and U251 cells were seeded in a 96-well plate with 100 cells/well. The culture plate was pre-cultured at 37°C in a 5% CO_2 incubator for 24 h. Then, the 10 μL CCK8 solution was added to each well. The culture plate was incubated in an incubator for 4 h. Absorbance at 450 nm was determined by an enzyme marker.[25]

2.8 | Flow cytometry

The U87 mg and U251 cells transfected with OE-NC, mimic NC, OE-NC + mimic NC, MIR4435-2HG-OE + mimic NC, or MIR4435-2HG-OE + miR-125a-5p were inoculated in a 60 mm cell culture dish at a density of 4×10^5 cells per well. After 24 h of culture, the cells were digested with trypsin and collected. The remaining cells were washed once with 1 ml PBS buffer. All of the cells were added to a 15-ml tube. After centrifugation at 800 rpm for 5 min, the supernatant was removed, and 5 ml PBS buffer was added to resuspend the cells, which were again centrifuged. The supernatant was discarded. This was repeated twice. Finally, the cells were resuspended in 0.5 ml PBS. Then, 5 ml of precooled 70% ethanol were added. The cells were shaken at 4°C overnight on a low-speed oscillator to fix. The next day, the fixed cells were centrifuged at 1000 rpm for 5 min, the supernatant was discarded, 4 ml PBS were added for cleaning once, and the cells were resuspended with 0.4 ml PBS. Then, 5 μl RNase A (10 mg/ml) was added for digestion at 37°C for 1 h, and the final concentration of 50 mg/ml propidium iodide (PI) was added for overnight staining at 4°C or 1 h at 37°C. The results were analyzed by epics XL flow cytometry.[26]

2.9 | Transwell test

Diluted with BD Matrigel 1:8, the upper surface of the bottom membrane of a transwell chamber was coated at 37°C for 30 min to polymerize the Matrigel into gels. The basement membrane was hydrated before use. The cell suspension was prepared. The transfected U87 MG cells and U251 cells were digested. After digestion, the cells were centrifuged, and the medium discarded. The cells were washed with PBS 1–2 times and resuspended in serum-free medium containing BSA. The cell density was adjusted to 5×10^5 cells/ml. Then, 100 μl of the cell suspension was removed and added to a transwell cell chamber. Generally, 600 μl medium containing 20% FBS was added into the lower chamber of a 24-well plate. Cells were cultured for 24 h. "Adherent" cells were counted. By staining the cells, the cells could be counted under a microscope. The transwell cells were removed, and the culture liquid in the hole was discarded. The cells were washed twice with PBS without calcium and fixed with methanol for 30 min. Then, 0.1% crystal violet was used to stain for 20 min. The upper layer of cells was washed 3 times with PBS. Under a 400× microscope, cells were observed in five visual fields and counted with photographs.[27]

2.10 | Clone formation test

Transfected U87 MG and U251 cell monolayers were digested with 0.25% trypsin, and the cells were separated into single cells by pipetting. The cells were suspended in RPMI 1640 medium supplemented with 10% fetal bovine serum. The cell suspension was diluted and inoculated into culture dishes at an appropriate cell density. Generally, 50, 100, and 200 cells were inoculated into dishes containing 10 ml 37°C preheated culture medium and gently rotated to make the cells disperse evenly. The cells were cultured for 2–3 weeks under the conditions of 37°C, 5% CO_2, and saturated humidity. When a visible clone was observed in the culture dish, the culture was terminated. The supernatant was discarded, and the cells were washed twice with PBS. Then, 5 ml of pure methanol or 1:3 acetic acid/methanol was added for 15 min to fix the cells. The fixative was then removed, and a proper amount of Giemsa dye was added for 10–30 min. The dye solution was then washed away with slowly running water. The cells were allowed to air dry. The plate was turned upside down, and a piece of transparent film with a grid was added. The clones were counted directly with the naked eye. Alternatively, clones with more than 10 cells were counted under a microscope (low power microscope). Finally, the clone formation rate was calculated. Clone formation rate = (number of clones)/number of inoculated cells × 100%.[28]

2.11 | Tumor implantation

Male Fischer rats (250–275 g) were used for this study. A 2-mm diameter craniotomy was opened on the right hemisphere anterior to the coronal suture. Using a Hamilton syringe, cells were injected 3.5 mm deep, 3.0 mm to the right, and 1.0 mm anterior of the bregma. Rats were implanted with 2.5×10^5 9L cells (5 μl PBS) over a 15-min interval. The craniotomy was covered with Horsley's bone wax, and the incision was closed with a 4–0 silk suture (Ethicon). A 5 μl of the mimic NC, OE-NC, miR-125a-5p mimic, TAZ-OE, inhibitor NC, sh-NC, miR-125a-5p inhibitor, or sh-TAZ was injected into each animal via intra-tumor injection at 5 days after tumor implantation. Using a Hamilton syringe, exosome suspension or PBS vehicle was injected at the same coordinates as the tumor implant, over a 5-min interval. Rats were sacrificed 10 days after implantation under anesthesia with i.p. administration of ketamine (100 mg/kg) and xylazine (10 mg/kg), the tumor volume was measured, and 250 μl whole blood were collected.[29]

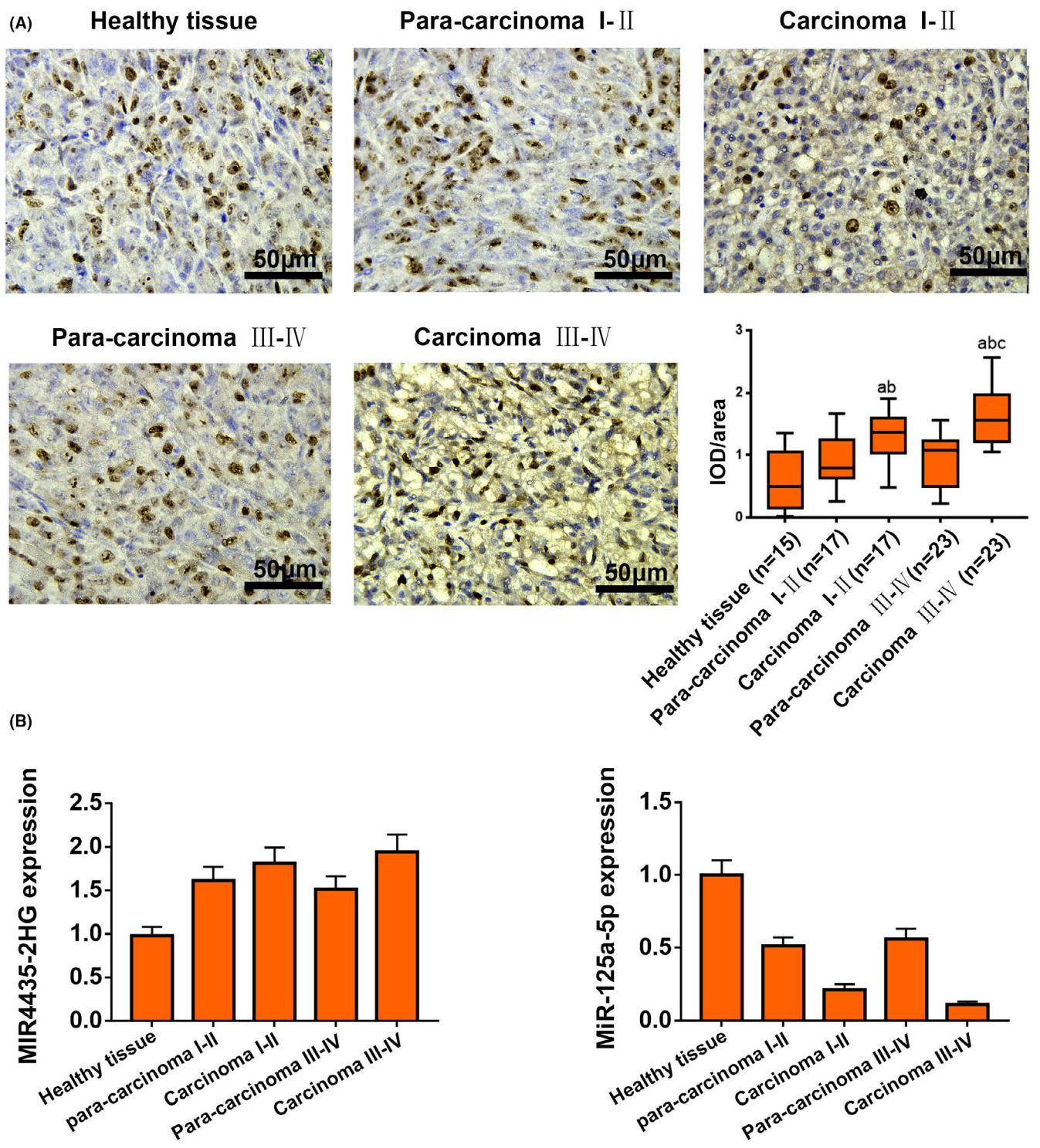

FIGURE 1 TAZ expression was high in the brain tissue of glioma patients, and it was higher in stage III-IV patients than in stage I-II patients. (A) Healthy brain tissue and glioma tissue were sectioned using a pathological section machine, embedded, and fixed. After incubation and staining with TAZ primary antibody, the expression of TAZ in the pathological tissues was obtained. The staining color of glioma tissue was significantly darker than that of healthy brain tissue, and the staining color of I-II cancer tissue and III-IV cancer tissue was significantly darker than that of corresponding paracancerous tissue. $^{a}p < 0.05$ vs healthy tissue, $^{b}p < 0.05$ vs para-carcinoma, $^{c}p < 0.05$ vs I-II. (B) MIR4435-2HG in glioma tissue was significantly higher than that in healthy brain tissue, miR-125a-5p was significantly lower than that in healthy brain tissue, MIR4435-2HG levels in stage I–II cancer tissue and stage III–IV cancer tissue were significantly higher than that in the corresponding paracancerous tissue, miR-125a-5p was significantly lower than that in corresponding paracancerous tissue, and MIR4435-2HG levels in stage III–IV patients were significantly higher than those in stage I–II patients, and miR-125a-5p levels in stage III–IV patients were significantly lower than those in stage I–II patients. $^{a}p < 0.05$ vs healthy tissue, $^{b}p < 0.05$ vs para-carcinoma, $^{c}p < 0.05$ vs I-II

2.12 | Statistical analysis

In this study, a preliminary experiment was carried out first, and a formal experiment was carried out after obtaining reliable results. In the formal experiment, each trial was performed at least three times, and all data are expressed as the mean ± standard deviation. For comparison of three or more data, one-way analysis of variance was adopted, and then Tukey's multiple comparison test was conducted. This study used GraphPad Prism 7.0 (GraphPad Software, Inc., San Diego, CA, USA) for statistical analysis.[30]

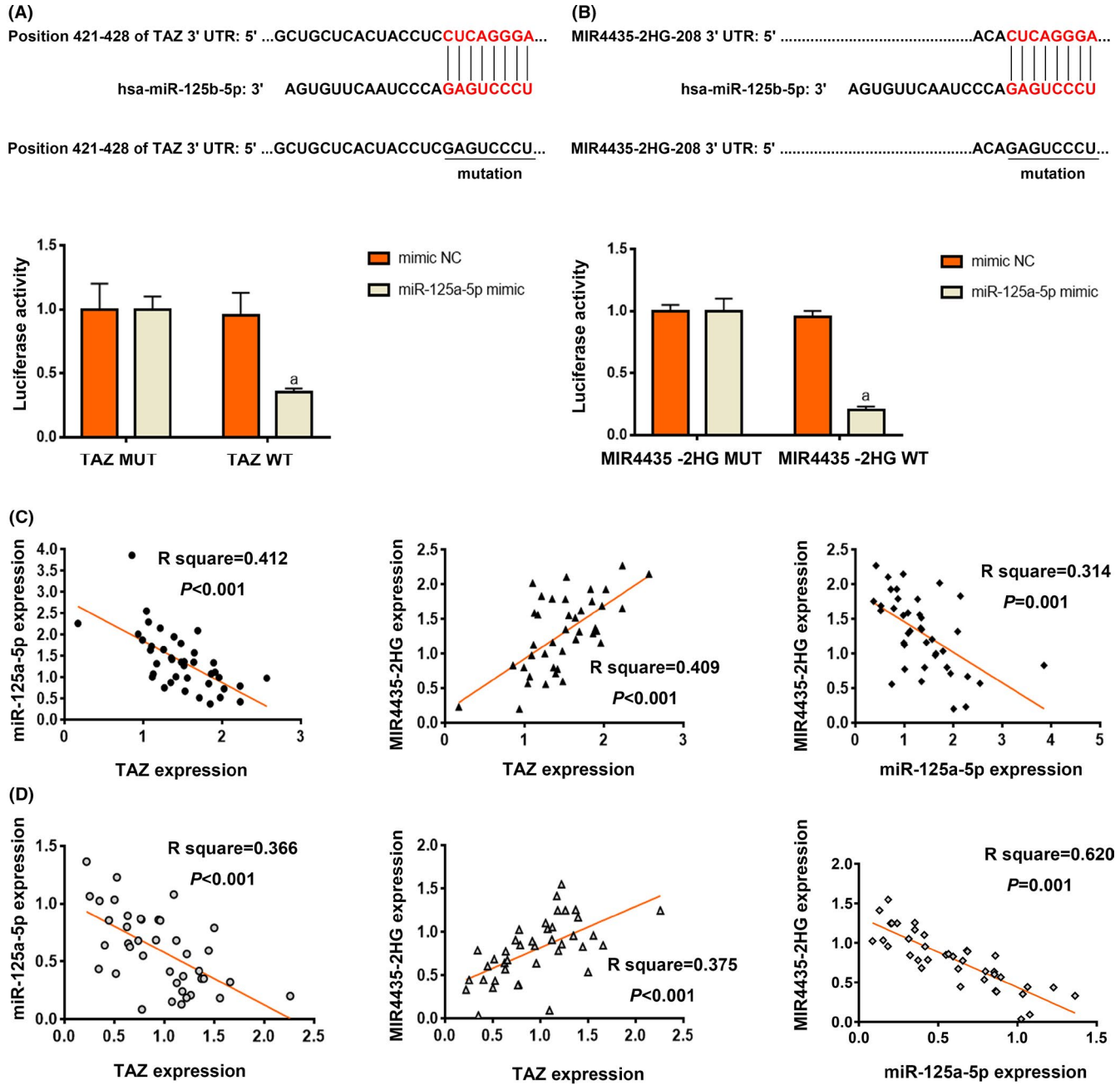

FIGURE 2 MIR4435-2HG was positively correlated with TAZ, and miR-125a-5p was negatively correlated with TAZ. (A,B) We used luciferase reporter assays to analyze the interactions between MIR4435-2HG and miR-125a-5p, miR-125a-5p, and TAZ. When there was a strong interaction between them, the activity of luciferase decreased. Mimic NC was used as a negative control. Compared with the TAZ wild-type miR-125a-5p mimic, the luciferase activity of the TAZ mutant was significantly higher. MIR4435-2HG and miR-125a-5p in the wild type have a strong relationship. Mic NC was used as a negative control. Compared with the MIR4435-2HG wild-type miR-125a-5p mimic, the luciferase activity of the MIR4435-2HG mutant was significantly higher. miR-125a-5p and TAZ in the wild type have a strong relationship. [a]$p < 0.05$ vs mimic NC. (C,D) We used *Pearson's* test (SPSS 25.0) to analyze the correlation between MIR4435-2HG and miR-125a-5p, miR-125a-5p, and TAZ. (C) indicates the carcinoma tissues of the glioma and (D) indicates the para-carcinoma tissues of the glioma. The continuous variables were plotted and the trend line was drawn. We found that MIR4435-2HG was positively correlated with TAZ, $p < 0.01$, miR-125a-5p was negatively correlated with TAZ, $p < 0.01$, and MIR4435-2HG was negatively correlated with miR-125a-5p, $p = 0.01$

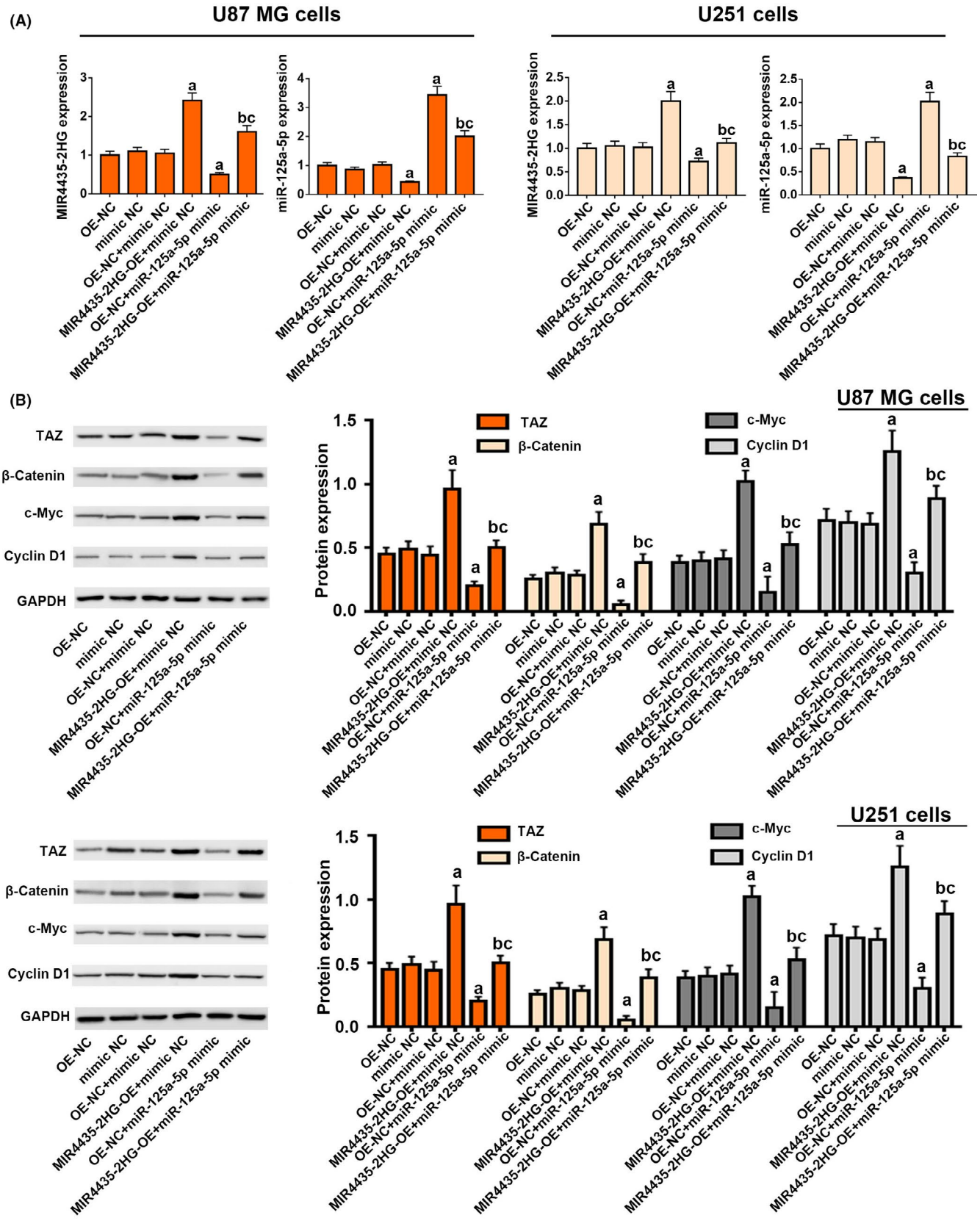
(A)
U87 MG cells
U251 cells
MIR4435-2HG expression
miR-125a-5p expression
OE-NC
mimic NC
OE-NC+mimic NC
MIR4435-2HG-OE+mimic NC
OE-NC+miR-125a-5p mimic
MIR4435-2HG-OE+miR-125a-5p mimic
(B)
TAZ
β-Catenin
c-Myc
Cyclin D1
GAPDH
Protein expression
U87 MG cells
U251 cells

FIGURE 3 MIR4435-2HG-OE can increase the expression of the TAZ gene and the expression of downstream genes of the cell proliferation signaling pathway Wnt. MiR-125a-5p inhibited the expression of the TAZ gene and the expression of the downstream genes of Wnt. The simultaneous action of MIR4435-2HG-OE and miR-125a-5p resulted in unaffected expression of the TAZ gene and the downstream genes of Wnt. (A) We used RT-qPCR to observe the expression levels of MIR4435-2HG-OE or miR-125a-5p in the U87 MG cells and U251 cells transfected with MIR4435-2HG-OE and miR-125a-5p, and confirmed that the transfection was successful. After transfection with MIR4435-2HG-OE, the expression level of MIR4435-2HG-OE in the two cell types was significantly increased, while the expression level of miR-125a-5p was significantly decreased. After transfection with miR-125a-5p, the expression level of miR-125a-5p in the two cell types was significantly increased, while the expression level of MIR4435-2HG-OE was significantly decreased. [a]$p < 0.05$ vs OE-NC/mimic NC, [b]$p < 0.05$ vs MIR4435-2HG-OE + mimic NC, [c]$p < 0.05$ vs OE-NC + miR-125a-5p mimic. (B) Western blots were performed on the U87 MG cells and U251 cells transfected with MIR4435-2HG-OE and miR-125a-5p, and the expression levels of the TAZ gene and the downstream genes of the Wnt signaling pathway, such as β-catenin, c-myc, and cyclin D1, were observed. The expression levels of the TAZ gene and downstream genes of the Wnt signaling pathway were significantly increased in the U87 MG and U251 cells transfected with MIR4435-2HG-OE. The expression levels of the TAZ gene and downstream genes of the Wnt signaling pathway in the U87 MG cells and U251 cells transfected with miR-125a-5p were significantly reduced or were even almost non-existent. The TAZ gene and the downstream genes of the Wnt signaling pathway in U87 MG cells and U251 cells transfected with MIR4435-2HG-OE and miR-125a-5p maintained low expression and no low expression. [a]$p < 0.05$ vs OE-NC/mimic NC, [b]$p < 0.05$ vs MIR4435-2HG-OE + mimic NC, [c]$p < 0.05$ vs OE-NC + miR-125a-5p mimic

3 | RESULTS

3.1 | Expressions of TAZ and MIR4435-2HG were high in the brain tissue of glioma patients; miR-125a-5p expression was low in the brain tissue of glioma patients

Healthy brain tissues and glioma tissues from patients collected between December 2017 and December 2018 were sectioned, embedded, and fixed. After incubating and staining with TAZ primary antibody, the expression of TAZ in the pathological tissues was obtained and was higher in stage III–IV patients than in stage I–II. The expressions of MIR4435-2HG and miR-125a-5p in the healthy brain tissues and glioma tissues were detected by RT-qPCR. The immunohistochemistry results showed that the glioma tissue staining was significantly darker than that of healthy brain tissue, and the staining colors of stage I–II cancer tissues and stage III–IV cancer tissues were significantly darker than those of corresponding paracancerous tissues. Mir4435-2HG levels in the glioma tissues were significantly higher than those in healthy brain tissues, mir-125a-5p levels were significantly lower than those in healthy brain tissues, mir4435-2HG levels in stage I–II cancer tissues and stage III–IV cancer tissues were significantly higher than those in corresponding paracancerous tissues, mir-125a-5p levels were significantly lower than those in corresponding paracancerous tissues, and mir4435-2HG levels in stage III–IV patients were significantly higher than those in stage I–II patients, and mir-125a-5p levels in stage III–IV patients were significantly lower than those in stage I–II patients (Figure 1, [a]$p < 0.05$ vs. healthy tissue, [b]$p < 0.05$ vs. para-carcinoma, [c]$p < 0.05$ vs. I–II).

TABLE 1 Relationship between TAZ expression and clinicopathological characteristics of patients with neuroglioma

Clinicopathological characteristics	*n*	TAZ expression	*p* value
Age (year)			
<60	23	1.503 ± 0.434	>0.05
≧60	17	1.462 ± 0.468	
Gender			
Male	21	1.472 ± 0.437	>0.05
Female	19	1.501 ± 0.464	
Tumor size (cm)			
<2.5	28	1.460 ± 0.441	>0.05
≧2.5	12	1.545 ± 0.463	
Tumor location			
Supratentorial gliomas	25	1.510 ± 0.427	>0.05
Infratentorial gliomas	15	1.447 ± 0.485	
Edema			
Present	10	1.539 ± 0.416	>0.05
Absent	30	1.468 ± 0.458	
Neoplasms histologic type			
Neuroastrocytoma	26	1.406 ± 0.470	>0.05
Oligodendroglioma	14	1.634 ± 0.357	
WHO grade			
I–II	17	1.303 ± 0.426	<0.05
III–IV	23	1.601 ± 0.469	

Abbreviation: WHO, World Health Organization.

3.2 | MIR4435-2HG correlated positively with TAZ; miR-125a-5p correlated negatively with TAZ

The luciferase reporter assay results indicated that, compared with TAZ wild-type miR-125a-5p mimic, the luciferase activity of the TAZ mutant was significantly higher. Mimic NC was used as the negative control. Compared with MIR4435-2HG wild-type miR-125a-5p mimic, the luciferase activity of the MIR4435-2HG mutant was significantly higher (Figure 2A,B, [a]$p < 0.05$ vs. mimic NC group). The expression level of MIR4435-2HG, miR-125a-5p, and TAZ in cancerous and paracancerous tissues of patients (the detailed clinical data of these patients were shown in Table 1) were determined. We used Pearson's test in SPSS 25.0 to analyze the correlation between MIR4435-2HG and miR-125a-5p and between miR-125a-5p and

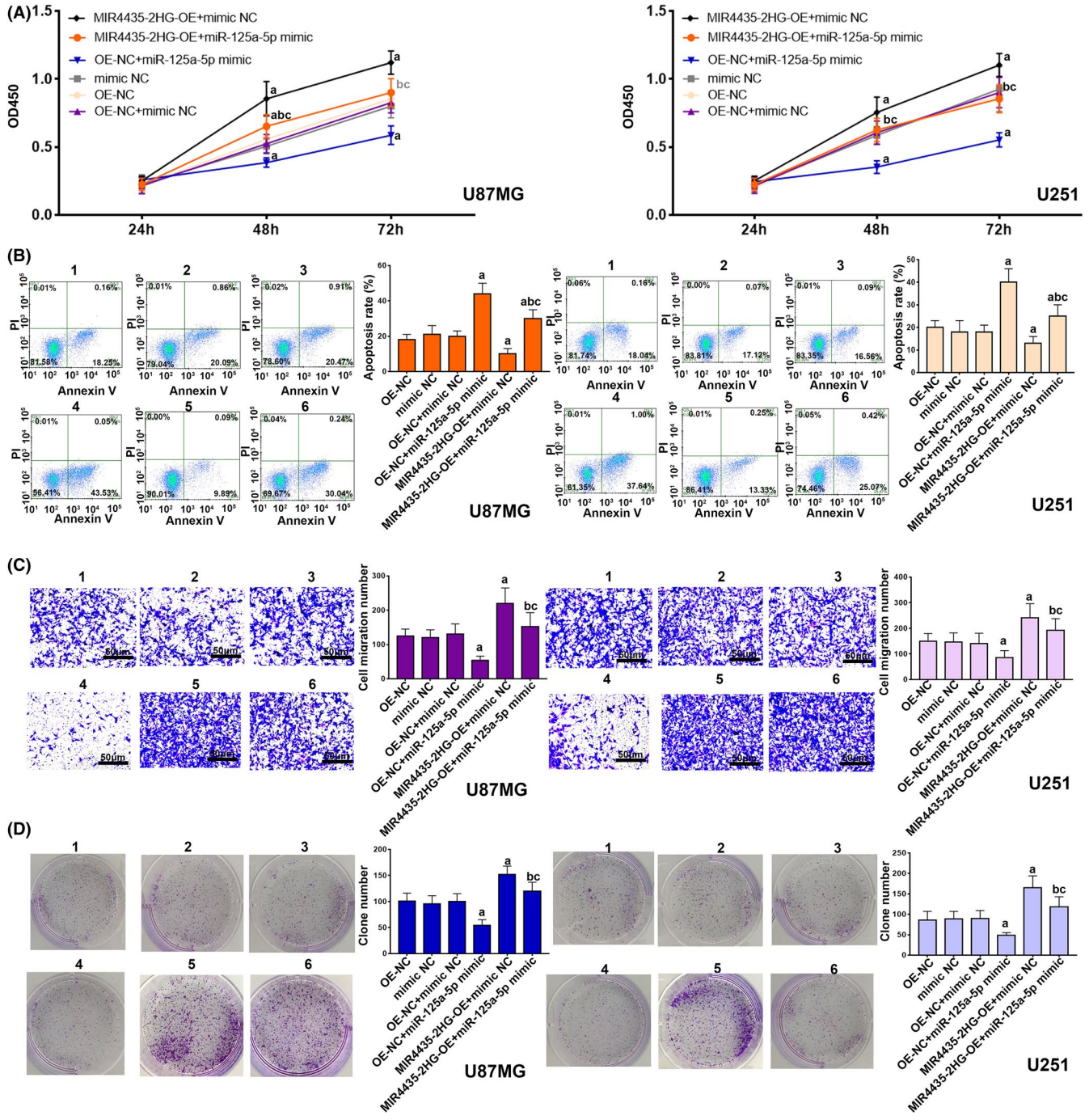

FIGURE 4 MIR4435-2HG-OE can improve the activities of U87 MG cells and U251 cells and inhibit apoptosis. MiR-125a-5p decreased the activity of the U87 MG cells and U251 cells, and promoted apoptosis. (A) We used the CCK8 test to detect the activity of glioma cells. The OD450 values of the U87 MG cells and U251 cells transfected with MIR4435-2HG-OE were the highest, and those of the U87 MG cells and U251 cells transfected with miR-125a-5p were the lowest. Meanwhile, the OD450 values of the U87 MG cells and U251 cells transfected with MIR4435-2HG-OE and miR-125a-5p were similar to those of the control liposomes. (B) We used flow cytometry to detect the apoptosis of glioma cells affected by MIR4435-2HG-OE or miR-125a-5p. The apoptosis of U87 MG cells and U251 cells transfected with MIR4435-2HG-OE was the least, and that of U87 MG cells and U251 cells transfected with miR-125a-5p was the most. The apoptosis of U87 MG cells and U251 cells transfected with MIR4435-2HG-OE and miR-125a-5p was similar to that of the control liposomes. (C) We used the transwell test to detect the migration of glioma cells. The migration of U87 MG cells and U251 cells transfected with MIR4435-2HG-OE was the most, and the migration of U87 MG cells and U251 cells transfected with miR-125a-5p was the least. The migration of U87 MG cells and U251 cells transfected with MIR4435-2HG-OE and miR-125a-5p was similar to that of the control liposomes. (D) Cell viability of U87 MG cells and U251 cells was detected by clonogenic assay. The number of clones formed of the U87 MG cells and U251 cells transfected with MIR4435-2HG-OE was the most, and that of the U87 MG cells and U251 cells transfected with miR-125a-5p was the least, while that of the U87 MG cells and U251 cells transfected with MIR4435-2HG-OE and miR-125a-5p was similar to that of the control liposomes. [a]$p < 0.05$ vs OE-NC/mimic NC, [b]$p < 0.05$ vs MIR4435-2HG-OE + mimic NC, [c]$p < 0.05$ vs OE-NC + miR-125a-5p mimic

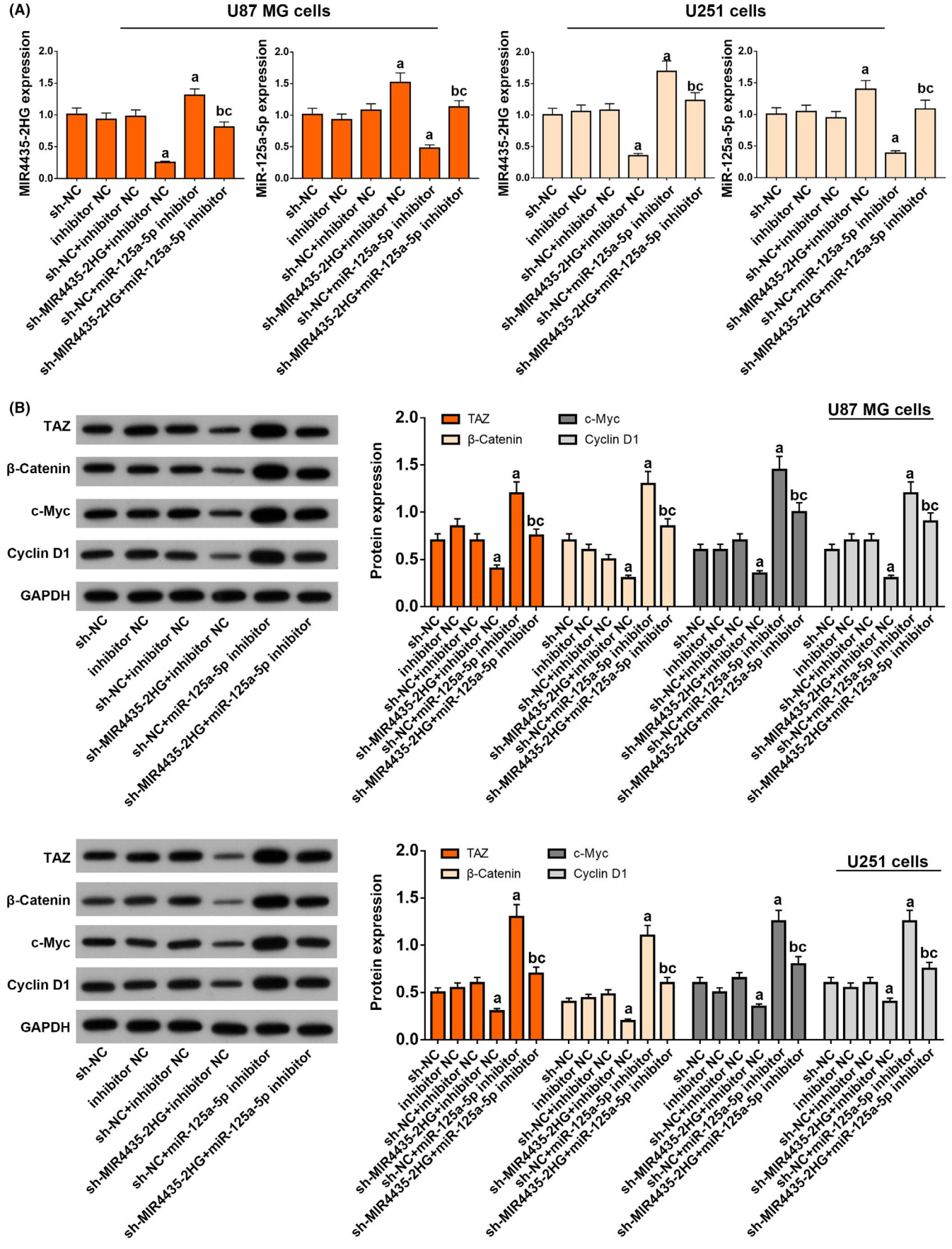
(A)
U87 MG cells
U251 cells
MIR4435-2HG expression
MiR-125a-5p expression
sh-NC
inhibitor NC
sh-NC+inhibitor NC
sh-MIR4435-2HG+inhibitor NC
sh-NC+miR-125a-5p inhibitor
sh-MIR4435-2HG+miR-125a-5p inhibitor
(B)
TAZ
β-Catenin
c-Myc
Cyclin D1
GAPDH
Protein expression
U87 MG cells
U251 cells

FIGURE 5 sh-MIR4435-2HG inhibited the expression of the TAZ gene and downstream genes of the Wnt signaling pathway. miR-125a-5p inhibitor increased the expression of the TAZ gene and expression of the downstream genes of Wnt. (A) RT-qPCR results showed that the expression levels of sh-MIR4435-2HG and miR-125a-5p inhibitor in U87 MG cells and U251 cells transfected with MIR4435-2HG and miR-125a-5p were inhibited, and the transfection was successful. After transfection with sh-MIR4435-2HG, the expression level of MIR4435-2HG in the two cell lines was significantly decreased, while the expression level of miR-125a-5p was significantly increased. After transfection with miR-125a-5p inhibitor, the expression level of miR-125a-5p in the two cell lines was significantly decreased, while the expression level of MIR4435-2HG was significantly increased. $^{a}p < 0.05$ vs. sh-NC/inhibitor NC group, $^{b}p < 0.05$ vs. sh-MIR4435-2HG + inhibitor NC group, $^{c}p < 0.05$ vs. sh-NC + miR-125a-5p inhibitor group. (B) Western blot analysis showed that the expression levels of TAZ and the downstream genes of the Wnt signaling pathway were significantly decreased in U87 MG and U251 cells transfected with sh-MIR4435-2HG. The expression levels of TAZ and the downstream genes of the Wnt signaling pathway in the U87 MG cells and U251 cells transfected with miR-125a-5p inhibitor were significantly increased. TAZ and the downstream genes of the Wnt signaling pathway in U87 MG cells and U251 cells transfected with sh-MIR4435-2HG and miR-125a-5p inhibitor maintained high expression and no high expression. $^{a}p < 0.05$ vs. sh-NC/inhibitor NC group, $^{b}p < 0.05$ vs. sh-MIR4435-2HG + inhibitor NC group, $^{c}p < 0.05$ vs. sh-NC + miR-125a-5p inhibitor group

TAZ. The continuous variables were plotted, and the trend line was drawn. The results showed that MIR4435-2HG was positively correlated with TAZ ($p < 0.01$), miR-125a-5p was negatively correlated with TAZ ($p < 0.01$), and MIR4435-2HG was negatively correlated with miR-125a-5p ($p = 0.01$) (Figure 2C,D).

3.3 | MIR4435-2HG-OE increased the expression of the TAZ gene and downstream genes of the Wnt signaling pathway; miR-125a-5p inhibited the expression of the TAZ gene and expression of the downstream genes of Wnt

The RT-qPCR results showed that the expression levels of MIR4435-2HG-OE and miR-125a-5p in U87 MG cells and U251 cells transfected with MIR4435-2HG-OE and miR-125a-5p were increased, and the transfection was successful. After transfection with MIR4435-2HG-OE, the expression level of MIR4435-2HG-OE in the two cell lines was significantly increased, while the expression level of miR-125a-5p was significantly decreased. After transfection with miR-125a-5p, the expression level of miR-125a-5p in the two cell lines was significantly increased, while the expression level of MIR4435-2HG-OE was significantly decreased (Figure 3A. $^{a}p < 0.05$ vs. OE-NC/mimic NC group, $^{b}p < 0.05$ vs. MIR4435-2HG-OE + mimic NC group, $^{c}p < 0.05$ vs. OE-NC + miR-125a-5p mimic group). Western blot analysis showed that the expression levels of TAZ and the downstream gene of the Wnt signaling pathway were significantly increased in U87 MG and U251 cells transfected with MIR4435-2HG-OE. The expression levels of TAZ and downstream gene of the Wnt signaling pathway in U87 MG cells and U251 cells transfected with miR-125a-5p were significantly reduced. TAZ and the downstream gene of the Wnt signaling pathway in U87 MG cells and U251 cells transfected with MIR4435-2HG-OE and miR-125a-5p maintained low expression and no low expression (Figure 3B, $^{a}p < 0.05$ vs. OE-NC/mimic NC group, $^{b}p < 0.05$ vs. MIR4435-2HG-OE + mimic NC group, $^{c}p < 0.05$ vs. OE-NC + miR-125a-5p mimic group).

3.4 | MIR4435-2HG-OE improved the activity of the U87 MG cells and U251 cells and inhibited apoptosis; miR-125a-5p decreased the activity of the U87 MG cells and U251 cells and promoted apoptosis; MIR4435-2HG-OE weakened the effect of miR-125a-5p

Results of the CCK8 assay showed that the OD450 values of U87 MG cells and U251 cells transfected with MIR4435-2HG-OE were the highest, and those of U87 MG cells and U251 cells transfected with miR-125a-5p were the lowest. The OD450 values of U87 MG cells and U251 cells transfected with MIR4435-2HG-OE and miR-125a-5p were similar to those transfected with the control liposomes. (Figure 4A) Flow cytometry results indicated that apoptosis of U87 MG cells and U251 cells transfected with MIR4435-2HG-OE was the least, and that of U87 MG cells and U251 cells transfected with miR-125a-5p was the most. Apoptosis of U87 MG cells and U251 cells transfected with MIR4435-2HG-OE and miR-125a-5p was similar to that of the cells with control liposome. (Figure 4B) The transwell assay results showed that the migration of U87 MG cells and U251 cells transfected with MIR4435-2HG-OE was the most, and the migration of U87 MG cells and U251 cells transfected with miR-125a-5p was the least. The migration of U87 MG cells and U251 cells transfected with MIR4435-2HG-OE and miR-125a-5p was similar to that of cells with the control liposome (Figure 4C). The results of the clonogenic assay showed the U87 MG cells and U251 cells transfected with MIR4435-2HG-OE had the most clone formation, and the U87 MG cells and U251 cells transfected with miR-125a-5p had the least. Clone formation in U87 MG cells and U251 cells transfected with MIR4435-2HG-OE and miR-125a-5p was similar to cells with the control liposome (Figure 4D, $^{a}p < 0.05$ vs. OE-NC/mimic NC group, $^{b}p < 0.05$ vs. MIR4435-2HG-OE + mimic NC group, $^{c}P < 0.05$ vs. OE-NC + miR-125a-5p mimic group).

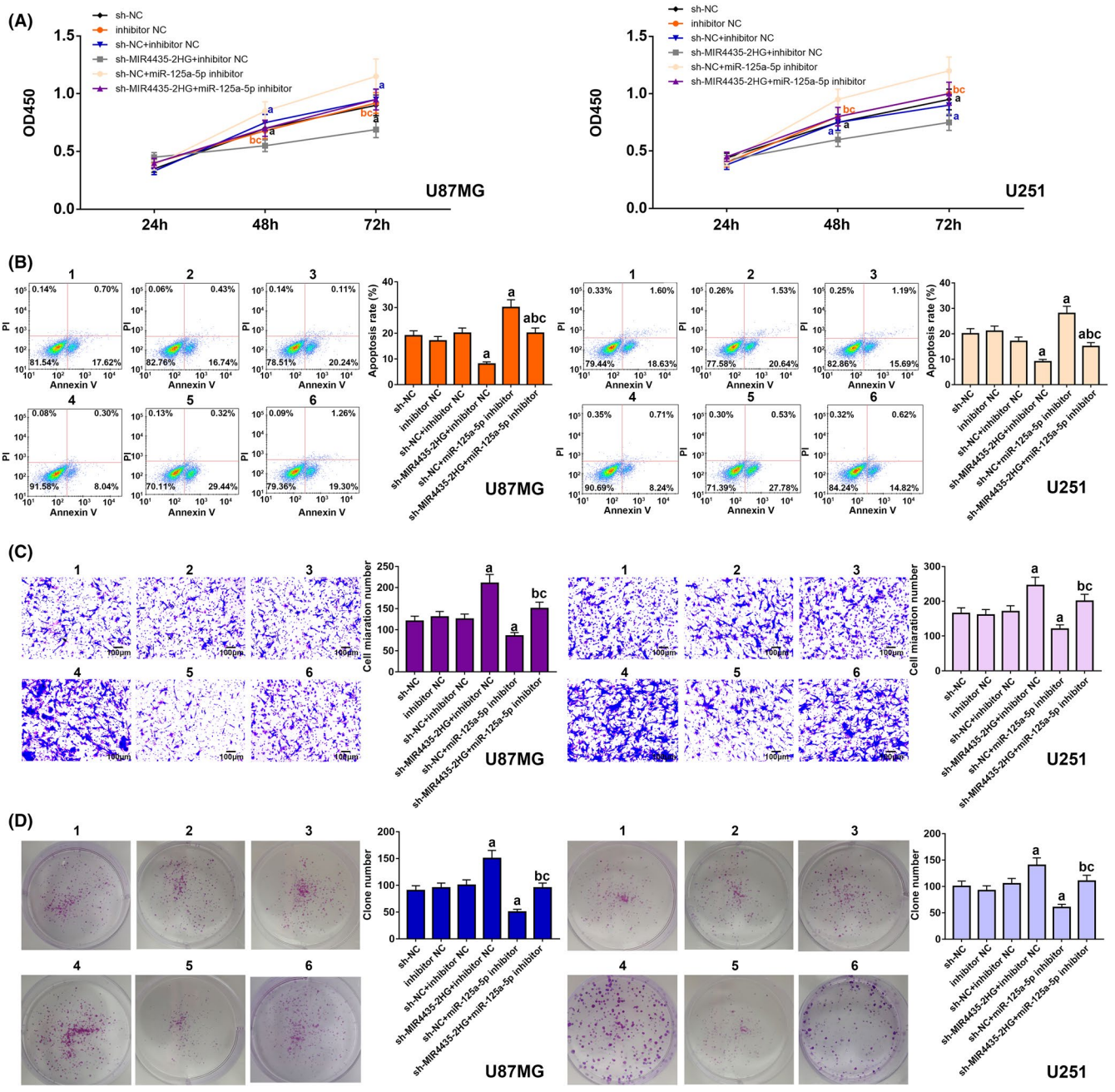

FIGURE 6 sh-MIR4435-2HG inhibited the activity of the U87 MG cells and U251 cells and improved apoptosis. miR-125a-5p inhibitor improved the activity of the U87 MG cells and U251 cells and inhibited apoptosis. sh-MIR4435-2HG weakened the effect of miR-125a-5p inhibitor. (A) Results of the CCK8 assay showed that the OD450 values of U87 MG cells and U251 cells transfected with sh-MIR4435-2HG were the lowest, and those of U87 MG cells and U251 cells transfected with miR-125a-5p inhibitor were the highest. The OD450 values of U87 MG cells and U251 cells transfected with sh-MIR4435-2HG and miR-125a-5p inhibitor were similar to those transfected with the control liposomes. (B) Flow cytometry results indicated that the apoptosis of U87 MG cells and U251 cells transfected with sh-MIR4435-2HG was the highest, and that of U87 MG cells and U251 cells transfected with miR-125a-5p inhibitor was the lowest. Apoptosis of U87 MG cells and U251 cells transfected with sh-MIR4435-2HG and miR-125a-5p inhibitor was similar to that of the cells with control liposomes. (C) Transwell assay results showed that the migration of U87 MG cells and U251 cells transfected with sh-MIR4435-2HG was the lowest, and the migration of U87 MG cells and U251 cells transfected with miR-125a-5p inhibitor was the highest. The migration of U87 MG cells and U251 cells transfected with sh-MIR4435-2HG and miR-125a-5p inhibitor was similar to that of cells with the control liposomes. D. Results of the clonogenic assay showed U87 MG cells and U251 cells transfected with sh-MIR4435-2HG had the least clone formation, and U87 MG cells and U251 cells transfected with miR-125a-5p inhibitor had the most. Clone formation in U87 MG cells and U251 cells transfected with sh-MIR4435-2HG and miR-125a-5p inhibitor was similar to cells with the control liposomes. [a]$p < 0.05$ vs. sh-NC/inhibitor NC group, [b]$p < 0.05$ vs. sh-MIR4435-2HG + inhibitor NC group, [c]$p < 0.05$ vs. sh-NC + miR-125a-5p inhibitor group

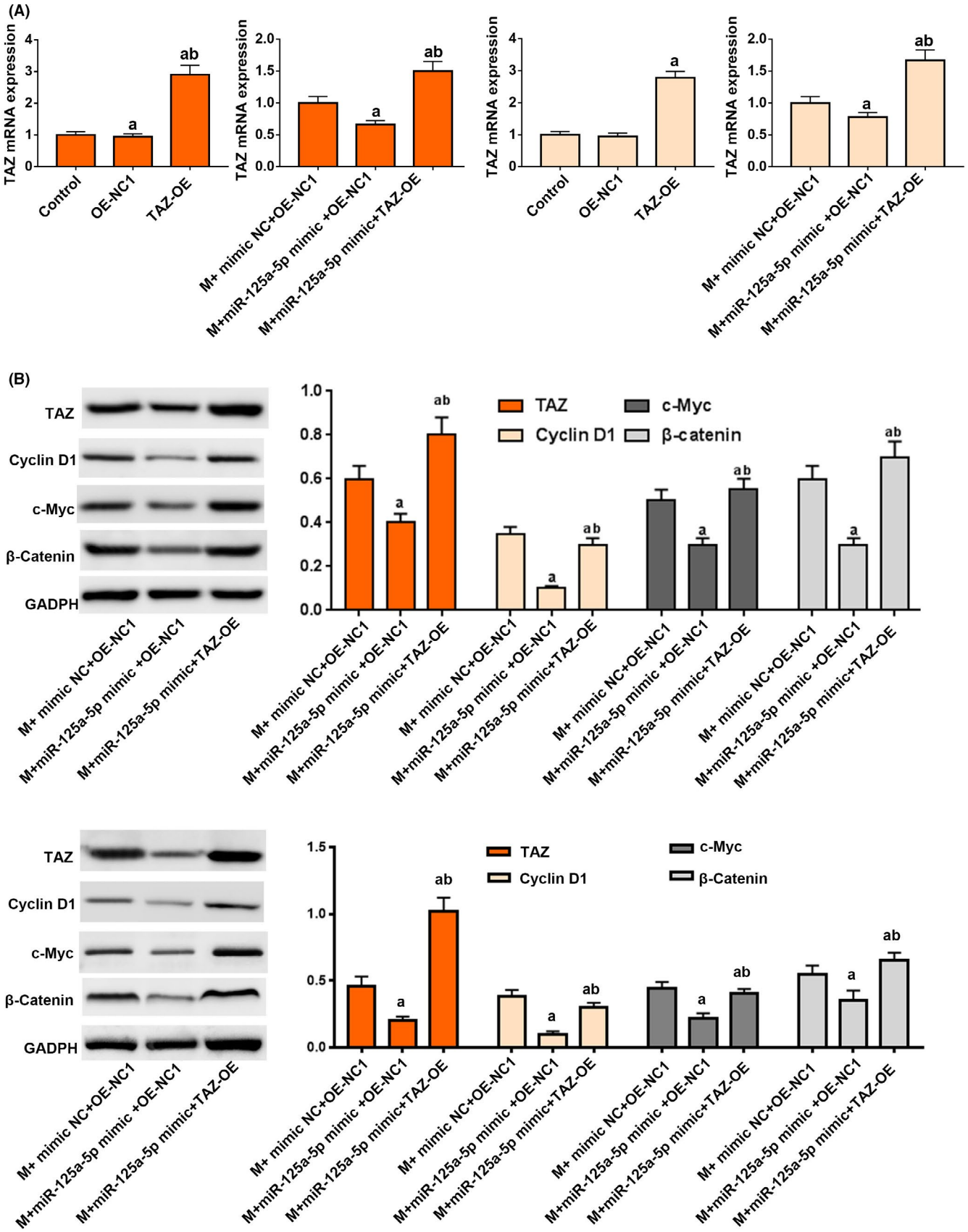
(A)
TAZ mRNA expression
Control
OE-NC1
TAZ-OE
M+ mimic NC+OE-NC1
M+miR-125a-5p mimic +OE-NC1
M+miR-125a-5p mimic+TAZ-OE
(B)
TAZ
Cyclin D1
c-Myc
β-Catenin
GADPH
β-catenin

FIGURE 7 Promoting effect of MIR4435-2HG on glioma cells was lower than the inhibitory effect of miR-125a-5p. The activation of the TAZ gene can promote the expression of downstream genes of the Wnt pathway. (A) We used RT-qPCR to detect whether U87 mg cells and U251 cells were successfully transfected with TAZ-OE and observed the expression of TAZ in combination with MIR4435-2HG, miR-125a-5p, and only MIR4435-2HG and miR-125a-5p. The results showed that TAZ-OE was successfully transfected, and the expression of TAZ in combination with MIR4435-2HG, miR-125a-5p only was significantly lower than that in the latter. (B) We used Western blotting to detect the expressions of TAZ and the Wnt downstream genes in the U87 mg cells and U251 cells. The results showed that the expression levels of TAZ, cyclin D1, c-myc, and β-catenin genes in U87 MG and U251 cells transfected with MIR4435-2HG and miR-125a-5p were significantly reduced. The expression levels of TAZ, cyclin D1, c-myc, and β-catenin genes in the cells transfected with MIR4435-2HG, miR-125a-5p, and TAZ-OE were significantly increased. M means MIR4435-2HG. $^{a}p < 0.05$ vs M + mimic NC + OE-NC1, $^{b}p < 0.05$ vs M + miR-125a-5p mimic + OE-NC1

3.5 | sh-MIR4435-2HG inhibited the expression of the TAZ gene and downstream genes of the Wnt signaling pathway; miR-125a-5p inhibitor increased the expression of the TAZ gene and the downstream genes of Wnt

The RT-qPCR results showed that the expression levels of sh-MIR4435-2HG and miR-125a-5p inhibitor in U87 MG cells and U251 cells transfected with MIR4435-2HG and miR-125a-5p were inhibited, and the transfection was successful. After transfection with sh-MIR4435-2HG, the expression level of MIR4435-2HG in the two cell lines was significantly decreased, while the expression level of miR-125a-5p was significantly increased. After transfection with miR-125a-5p inhibitor, the expression level of miR-125a-5p in the two cell lines was significantly decreased, while the expression level of MIR4435-2HG was significantly increased (Figure 5A. $^{a}p < 0.05$ vs. sh-NC/inhibitor NC group, $^{b}p < 0.05$ vs. sh-MIR4435-2HG + inhibitor NC group, $^{c}p < 0.05$ vs. sh-NC + miR-125a-5p inhibitor group). Western blot analysis showed that the expression levels of TAZ and the downstream genes of the Wnt signaling pathway were significantly decreased in the U87 MG and U251 cells transfected with sh-MIR4435-2HG. The expression levels of TAZ and the downstream genes of the Wnt signaling pathway in U87 MG cells and U251 cells transfected with miR-125a-5p inhibitor were significantly increased. TAZ and the downstream genes of the Wnt signaling pathway in the U87 MG cells and U251 cells transfected with sh-MIR4435-2HG and miR-125a-5p inhibitor maintained high expression and no high expression (Figure 5B, $^{a}p < 0.05$ vs. sh-NC/inhibitor NC group, $^{b}p < 0.05$ vs. sh-MIR4435-2HG + inhibitor NC group, $^{c}p < 0.05$ vs. sh-NC + miR-125a-5p inhibitor group).

3.6 | sh-MIR4435-2HG inhibited the activities of the U87 MG cells and U251 cells and improved apoptosis; miR-125a-5p inhibitor improved the activities of the U87 MG cells and U251 cells and inhibited apoptosis; sh-MIR4435-2HG weakened the effect of the miR-125a-5p inhibitor

Results of the CCK8 assay showed that the OD450 values of the U87 MG cells and U251 cells transfected with sh-MIR4435-2HG were the lowest, while those of the U87 MG cells and U251 cells transfected with miR-125a-5p inhibitor were the highest. The OD450 values of the U87 MG cells and U251 cells transfected with sh-MIR4435-2HG and miR-125a-5p inhibitor were similar to those transfected with the control liposomes (Figure 6A). Flow cytometry results indicated that the levels of apoptosis of the U87 MG cells and U251 cells transfected with sh-MIR4435-2HG were the highest, and those of the U87 MG cells and U251 cells transfected with miR-125a-5p inhibitor were the lowest. Apoptosis levels of the U87 MG cells and U251 cells transfected with sh-MIR4435-2HG and miR-125a-5p inhibitor were similar to those of the cells with control liposome (Figure 6B). The transwell assay results showed that the migration of the U87 MG cells and U251 cells transfected with sh-MIR4435-2HG was the least, and the migration of the U87 MG cells and U251 cells transfected with miR-125a-5p inhibitor was the most. The migration of the U87 MG cells and U251 cells transfected with sh-MIR4435-2HG and miR-125a-5p inhibitor was similar to that of cells with the control liposome (Figure 6C). The results of the clonogenic assay showed the U87 MG cells and U251 cells transfected with sh-MIR4435-2HG had the least clone formation, and the U87 MG cells and U251 cells transfected with miR-125a-5p inhibitor had the most clone formation. In U87 MG cells and U251 cells transfected with sh-MIR4435-2HG and miR-125a-5p inhibitor, the number of clones was similar to cells with the control liposome (Figure 6D. $^{a}p < 0.05$ vs. sh-NC/inhibitor NC group, $^{b}p < 0.05$ vs. sh-MIR4435-2HG + inhibitor NC group, $^{c}p < 0.05$ vs. sh-NC + miR-125a-5p inhibitor group).

3.7 | The promoting effect of MIR4435-2HG on glioma cells was less effective than the inhibitory effect of miR-125a-5p; TAZ and MIR4435-2HG had a synergistic effect

We used RT-qPCR to observe the expression of TAZ in combination with MIR4435-2HG, miR-125a-5p, and only MIR4435-2HG and miR-125a-5p. The results showed that TAZ-OE was successfully transfected, and the expression of TAZ in combination was significantly higher than that in groups not transfected with TAZ-OE. (Figure 7A). We used Western blotting to detect the expressions of TAZ and the Wnt downstream genes in U87 MG cells and U251 cells. The results showed that the expression levels of TAZ, cyclin D1, c-myc, and β-catenin in U87 MG and U251 cells transfected with MIR4435-2HG and miR-125a-5p were significantly reduced.

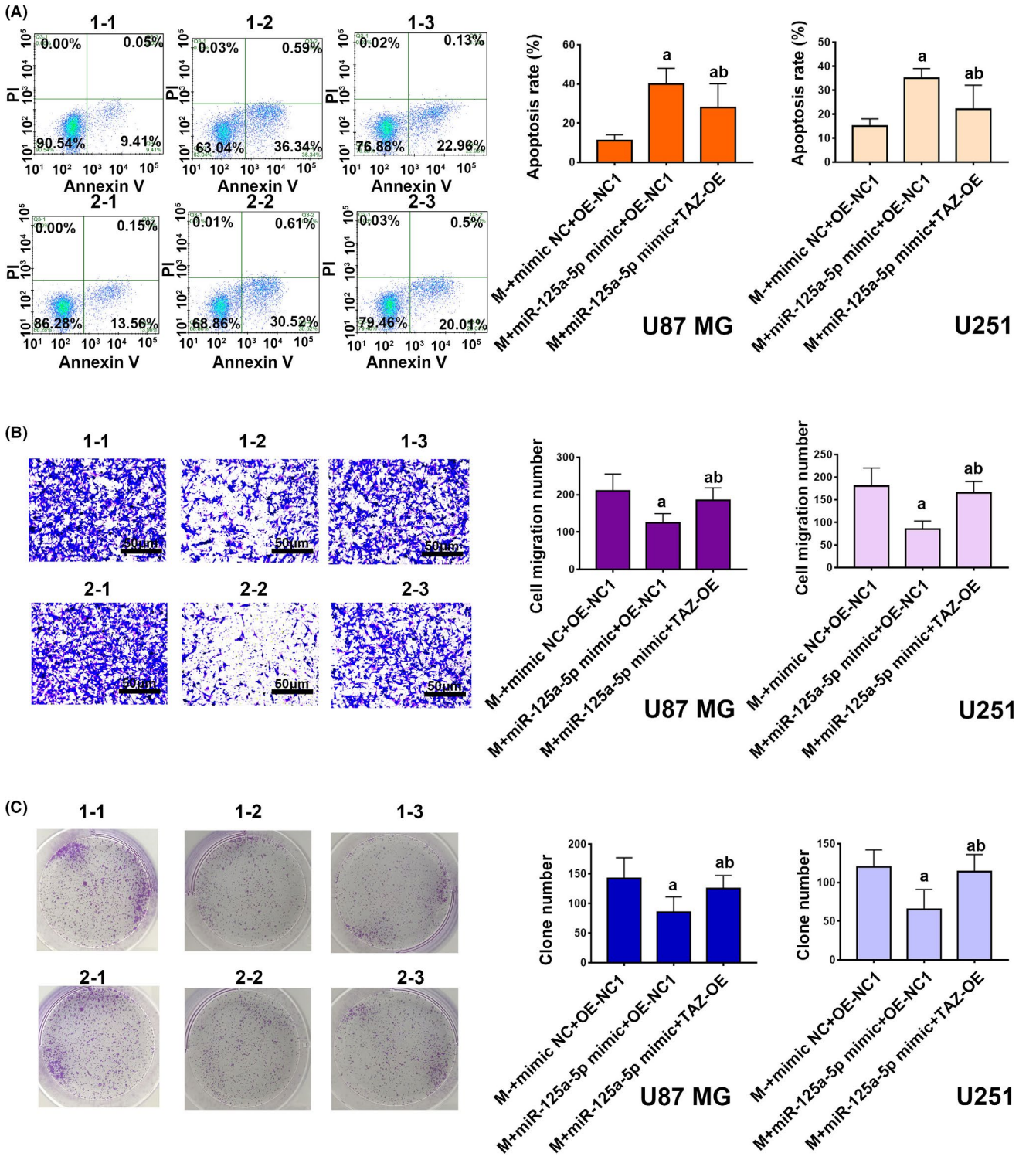

FIGURE 8 MIR4435-2HG and TAZ inhibited apoptosis and promoted cell migration and proliferation. MiR-125a-5p promoted cell apoptosis and inhibited cell migration and proliferation. (A) We used flow cytometry to detect the apoptosis of glioma cells. U87 MG cells and U251 cells transfected only with M had the least apoptosis. The apoptosis of U87 MG cells and U251 cells transfected with M and miR-125a-5p increased significantly, while that of cells transfected with M and miR-125a-5p and TAZ-OE decreased. (B) We used the transwell test to detect the migration and invasion of glioma cells. U87 MG cells and U251 cells transfected only with M had the strongest migration ability. The migration ability of U87 MG cells and U251 cells transfected with M and miR-125a-5p was significantly lower, while that of cells transfected with M and miR-125a-5p and TAZ-OE was somewhat higher but was less than that of cells transfected with M. (C) We used the clonogenesis assay to detect the proliferation of glioma cells. U87 MG cells and U251 cells transfected with M only proliferated most obviously and formed the most clones. The proliferation of U87 MG cells and U251 cells transfected with M and miR-125a-5p was significantly lower, while the proliferation of cells transfected with M and miR-125a-5p and TAZ-OE was somewhat higher but was less than that of the cells transfected only with M. M means MIR4435-2HG. $^{a}p < 0.05$ vs M + mimic NC + OE-NC1, $^{b}p < 0.05$ vs M + miR-125a-5p mimic + OE-NC1

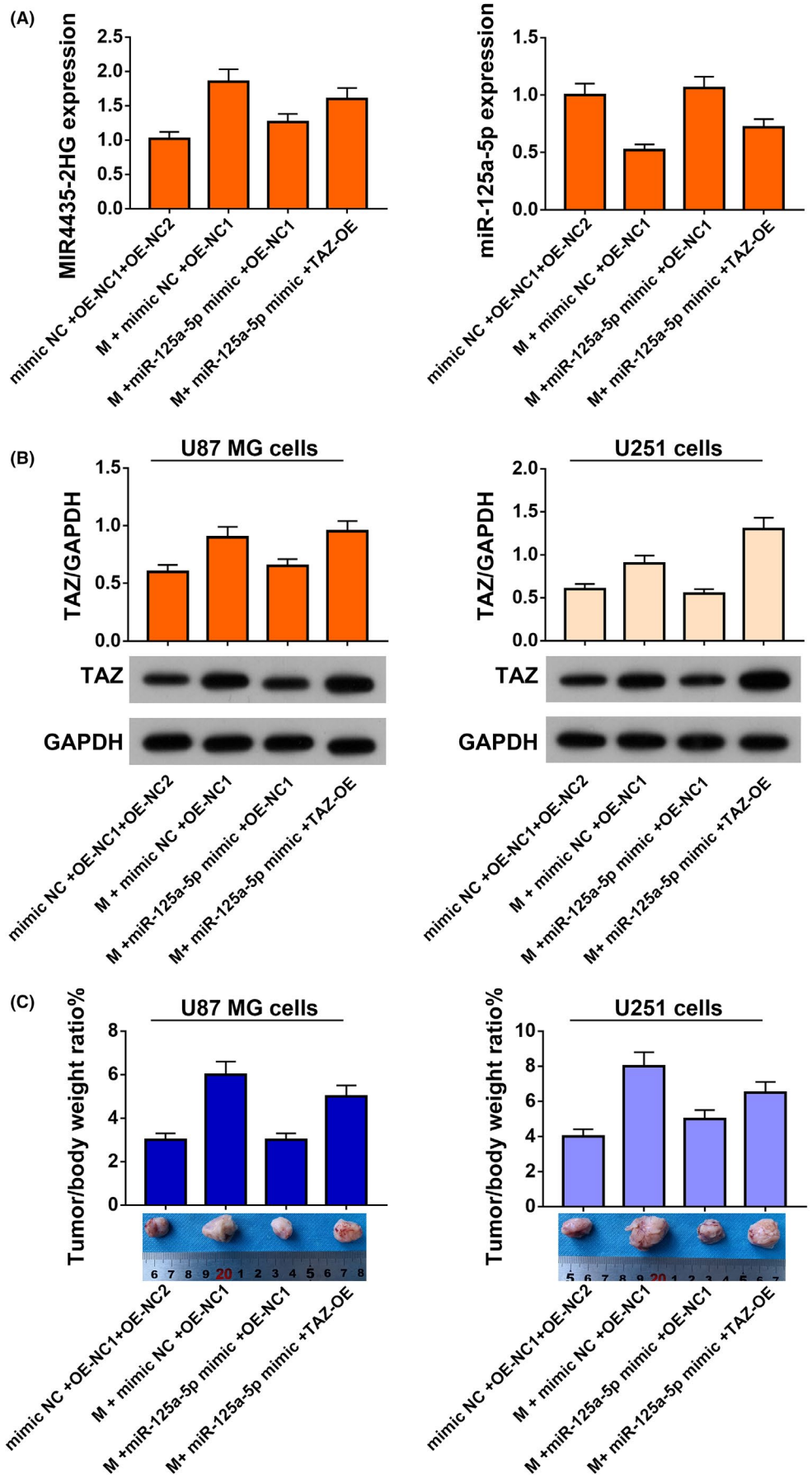
(A)
MIR4435-2HG expression
2.5
2.0
1.5
1.0
0.5
0.0
miR-125a-5p expression
1.5
1.0
0.5
0.0
mimic NC +OE-NC1+OE-NC2
M + mimic NC +OE-NC1
M +miR-125a-5p mimic +OE-NC1
M+ miR-125a-5p mimic +TAZ-OE
(B)
U87 MG cells
U251 cells
TAZ/GAPDH
TAZ
GAPDH
(C)
Tumor/body weight ratio%

FIGURE 9 Promoting effect of MIR4435-2HG on glioma rats was lower than the inhibitory effect of miR-125a-5p. TAZ and MIR4435-2HG had a synergistic effect. (A) We used RT-qPCR to observe the expression of TAZ in combination with MIR4435-2HG, miR-125a-5p, and only MIR4435-2HG and miR-125a-5p. The results showed that TAZ-OE was successfully transfected, and the expression of TAZ in combination with MIR4435-2HG and miR-125a-5p was significantly lower than that in the latter. (B) We used Western blotting to detect the expression of TAZ and the Wnt downstream genes in glioma rats. The results showed that the expression levels of TAZ, cyclin D1, c-myc, and β-catenin in glioma rats transfected with MIR4435-2HG and miR-125a-5p were significantly reduced. The expression levels of TAZ, cyclin D1, c-myc, and β-catenin in the cells transfected with MIR4435-2HG, miR-125a-5p, and TAZ-OE were significantly increased. (C) The tumor volumes of MIR4435-2HG and TAZ-OE groups were significantly increased, while those of the miR-125a-5p group were significantly decreased. $^{a}p < 0.05$ vs. mimic NC + OE-NC1 + OE-NC2 group, $^{b}p < 0.05$ vs. M + mimic NC + OE-NC1 group, $^{b}p < 0.05$ vs. M + miR-125a-5p mimic + TAZ-OE

The expression levels of TAZ, cyclin D1, c-myc, and β-catenin in the cells transfected with MIR4435-2HG, miR-125a-5p, and TAZ-OE were significantly increased (Figure 7B, $^{a}p < 0.05$ vs. MIR4435-2HG + mimic NC + OE-NC, group vs. M + miR-125a-5p mimic + OE-NC1 group; $^{b}p < 0.05$).

3.8 | MIR4435-2HG and TAZ inhibited apoptosis and promoted cell migration and proliferation; miR-125a-5p promoted cell apoptosis and inhibited cell migration and proliferation

We used flow cytometry to detect the apoptosis of glioma cells. U87 MG cells and U251 cells transfected only with MIR4435-2HG (M) had the least apoptosis. Cells transfected with both M and miR-125a-5p had significantly increased apoptosis compared with M + mimic NC + OE-NC1 group, while cells transfected with M and miR-125a-5p and TAZ-OE had decreased apoptosis compared with M + mimic NC + OE-NC1 group (Figure 8A). The transwell assay was used to detect the migration and invasion of glioma cells. U87 MG cells and U251 cells transfected with only M had the strongest migration ability compared with cells transfected with M and miR-125a-5p or transfected with M and miR-125a-5p and TAZ-OE. Cells transfected with M and miR-125a-5p had the weakest migration ability, while the migration ability of cells transfected with M and miR-125a-5p and TAZ-OE was increased (Figure 8B). The clonogenesis assay was used to detect proliferation of the glioma cells. U87 MG cells and U251 cells transfected with M only proliferated most obviously and formed the most clones. Proliferation of the U87 MG cells and U251 cells transfected with M and miR-125a-5p decreased significantly, while proliferation of the cells transfected with M and miR-125a-5p and TAZ-OE was increased (Figure 8C, $^{a}p < 0.05$ vs M + mimic NC + OE-NC1 group, $^{b}p < 0.05$ vs M + miR-125a-5p mimic + OE-NC1 group).

3.9 | Promoting effect of MIR4435-2HG on glioma rats was lower than the inhibitory effect of miR-125a-5p; TAZ and MIR4435-2HG had a synergistic effect

We used RT-qPCR to observe the expression of TAZ in combination with MIR4435-2HG, miR-125a-5p, and only MIR4435-2HG and miR-125a-5p. The results showed that MIR4435-2HG-OE was significantly increased, and the expression of miR-125a-5p decreased significantly (Figure 9A). We used Western blotting to detect the expressions of TAZ and the Wnt downstream genes in glioma rats. The results showed that the expression levels of TAZ, cyclin D1, c-myc, and β-catenin in glioma rats transfected with MIR4435-2HG and miR-125a-5p were significantly reduced. The expression levels of TAZ, cyclin D1, c-myc, and β-catenin in the cells transfected with MIR4435-2HG, miR-125a-5p, and TAZ-OE were significantly increased (Figure 9B). The tumor volume of the MIR4435-2HG and TAZ-OE group was significantly increased, while that of the miR-125a-5p group was significantly decreased (Figure 9C, $^{a}p < 0.05$ vs. mimic NC + OE-NC1 + OE-NC2 group, $^{b}p < 0.05$ vs. M + mimic NC + OE-NC1 group, $^{c}p < 0.05$ vs. M + miR-125a-5p mimic + TAZ-OE).

3.10 | Inhibitory effect of sh-MIR4435-2HG on glioma rats was lower than the promoting effect of miR-125a-5p inhibitor

We used RT-qPCR to observe the expression of TAZ in combination with MIR4435-2HG, miR-125a-5p, and only MIR4435-2HG and miR-125a-5p. The results showed that sh-MIR4435-2HG was successfully transfected, and the expression of MIR4435-2HG decreased significantly. sh-MIR4435-2HG and sh-TAZ have synergistic effect (Figure 10A). We used Western blotting to detect the expressions of TAZ and the Wnt downstream genes in glioma rats. The results showed that the expression levels of TAZ, cyclin D1, c-myc, and β-catenin in glioma rats transfected with sh-MIR4435-2HG and miR-125a-5p inhibitor were significantly increased. The expression levels of TAZ, cyclin D1, c-myc, and β-catenin in the cells transfected with sh-MIR4435-2HG, miR-125a-5p inhibitor, and sh-TAZ were significantly reduced (Figure 10B). The tumor volumes of the sh-MIR4435-2HG group and TAZ-OE group were significantly decreased, while that of the mir-125a-5p inhibitor group was significantly increased (Figure 10C, $^{a}p < 0.05$ vs. inhibitor NC + sh-NC1 + sh-NC2 group, $^{b}p < 0.05$ vs. M + inhibitor NC + sh-NC1 group, $^{c}p < 0.05$ vs. miR-125a-5p inhibitor + sh-NC1).

4 | DISCUSSION

Glioma is the most common central nervous system tumor, and it has a high malignancy and a high mortality rate.[31] At present, patients

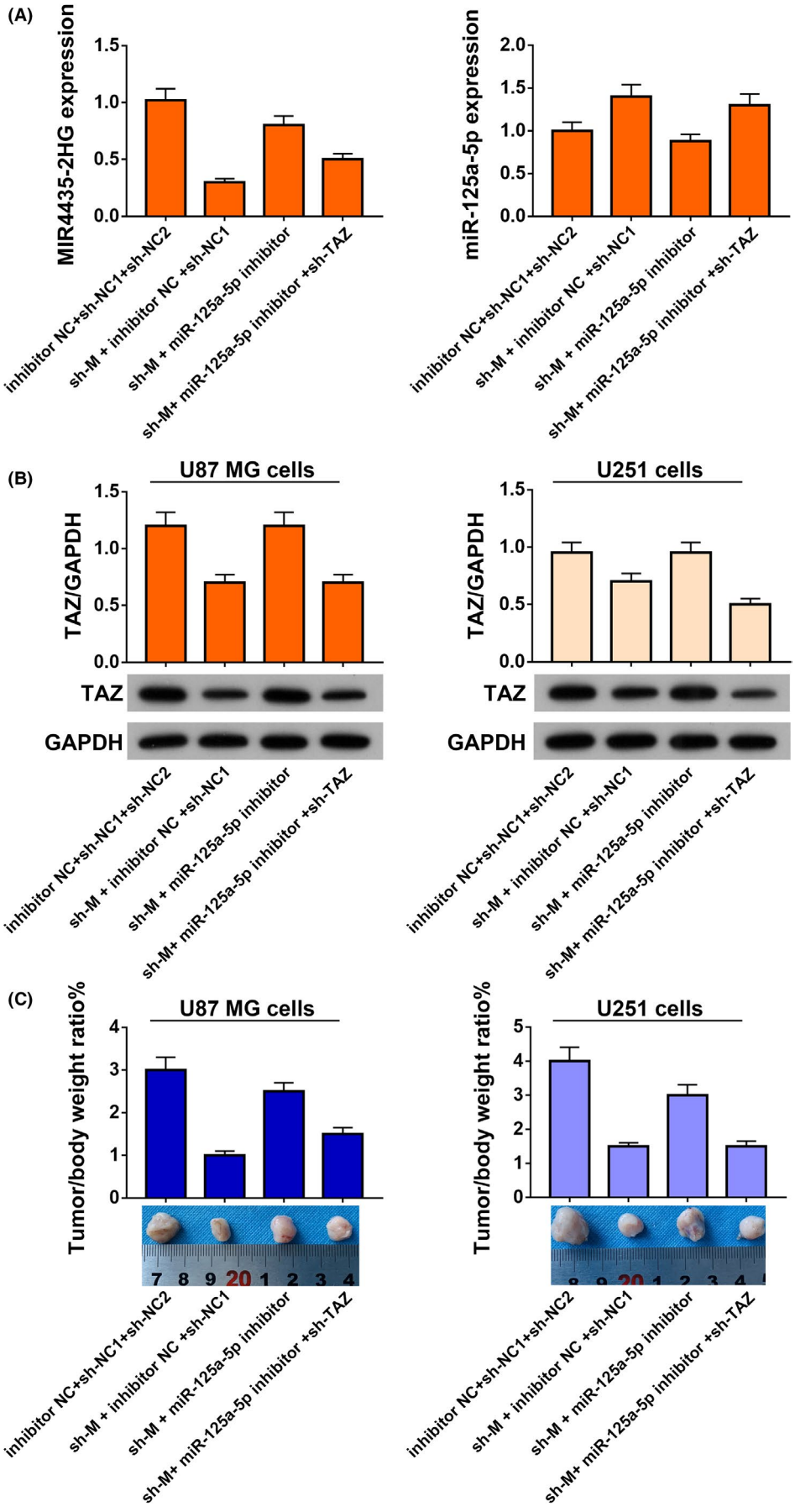
(A)
MIR4435-2HG expression
1.5
1.0
0.5
0.0
inhibitor NC+sh-NC1+sh-NC2
sh-M + inhibitor NC +sh-NC1
sh-M + miR-125a-5p inhibitor
sh-M+ miR-125a-5p inhibitor +sh-TAZ
miR-125a-5p expression
2.0
1.5
1.0
0.5
0.0
inhibitor NC+sh-NC1+sh-NC2
sh-M + inhibitor NC +sh-NC1
sh-M + miR-125a-5p inhibitor
sh-M+ miR-125a-5p inhibitor +sh-TAZ
(B)
U87 MG cells
TAZ/GAPDH
1.5
1.0
0.5
0.0
TAZ
GAPDH
inhibitor NC+sh-NC1+sh-NC2
sh-M + inhibitor NC +sh-NC1
sh-M + miR-125a-5p inhibitor
sh-M+ miR-125a-5p inhibitor +sh-TAZ
U251 cells
TAZ/GAPDH
1.5
1.0
0.5
0.0
TAZ
GAPDH
inhibitor NC+sh-NC1+sh-NC2
sh-M + inhibitor NC +sh-NC1
sh-M + miR-125a-5p inhibitor
sh-M+ miR-125a-5p inhibitor +sh-TAZ
(C)
U87 MG cells
Tumor/body weight ratio%
4
3
2
1
0
7 8 9 20 1 2 3 4
inhibitor NC+sh-NC1+sh-NC2
sh-M + inhibitor NC +sh-NC1
sh-M + miR-125a-5p inhibitor
sh-M+ miR-125a-5p inhibitor +sh-TAZ
U251 cells
Tumor/body weight ratio%
5
4
3
2
1
0
inhibitor NC+sh-NC1+sh-NC2
sh-M + inhibitor NC +sh-NC1
sh-M + miR-125a-5p inhibitor
sh-M+ miR-125a-5p inhibitor +sh-TAZ

FIGURE 10 Inhibitory effect of sh-MIR4435-2HG on glioma rats was lower than the promoting effect of miR-125a-5p inhibitor. (A) We used RT-qPCR to observe the expression of TAZ in combination with MIR4435-2HG, miR-125a-5p, and only MIR4435-2HG and miR-125a-5p. The results showed that sh-TAZ was successfully transfected, and the expression of TAZ in combination with MIR4435-2HG and miR-125a-5p was significantly higher than that in the latter. (B) We used Western blotting to detect the expressions of TAZ and the Wnt downstream genes in glioma rats. The results showed that the expression levels of TAZ, cyclin D1, c-myc, and β-catenin in glioma rats transfected with sh-MIR4435-2HG and miR-125a-5p inhibitor were significantly increased. The expression levels of TAZ, cyclin D1, c-myc, and β-catenin in the cells transfected with sh-MIR4435-2HG, miR-125a-5p inhibitor, and sh-TAZ were significantly reduced. (C) The tumor volumes of the sh-MIR4435-2HG and TAZ-OE groups were significantly decreased, while those of the miR-125a-5p inhibitor group were significantly increased. [a]$p < 0.05$ vs. inhibitor NC + sh-NC1 + sh-NC2 group, [b]$p < 0.05$ vs. M + inhibitor NC + sh-NC1 group, [b]$p < 0.05$ vs. miR-125a-5p inhibitor + sh-NC1

with primary gliomas are treated mainly by tumor resection, adjuvant radiotherapy, and periodic chemotherapy.[32] The blood-brain barrier is the main obstacle in the treatment of gliomas.[33] Although the standard treatment can improve the survival rate of patients, it easily leads to drug resistance of tumor tissues, and the treatment effect is poor.[34] Intracranial resection is also prone to recurrence.[35] Now, a therapeutic target and the mechanism of gliomas must be found so that effective new drugs can be developed.

Our research focused on the TAZ gene, which has been related to gliomas. We used biostatistics and experiments to find the possible mechanism of glioma development and confirmed it with cytology tests. Our results show that MIR4435-2HG correlated positively with TAZ, while miR-125a-5p correlated negatively with TAZ. MIR4435-2HG had an inhibitory effect on miR-125a-5p by promoting TAZ. Animal experiments also confirmed the relationship between the lncRNA MIR4435-2HG, miR-125a-5p, and TAZ. According to some studies,[36-38] expression of the TAZ gene can promote the development of gliomas. Tian et al.[38] studied first-line chemotherapy for glioblastoma multiforme (GBM). Their results showed that TAZ inhibits temozolomide-induced apoptosis by upregulating MCL-1 (myeloid cell leukemia 1) and that high expression of TAZ predicts poor prognosis for GBM patients. Li et al.[39] evaluated the expression of TAZ and its role in tumor invasion and metastasis in human gliomas. They found overexpression of TAZ protein in human gliomas and its elevated expression correlated significantly with poor differentiation. TAZ knockdown prominently reduces cell migration and invasion in SNB19 cells. Bhat et al.[40] showed that TAZ is directly recruited to a majority of mesenchymal (MES) gene promoters in a complex with TEA domain family member 2 (TEAD2). They uncovered a direct role for TAZ and TEAD in driving the MES differentiation of malignant gliomas.

There are still many deficiencies in our research that need to be addressed by researchers. All glioma cell lines should be tested. There are many kinds of gliomas, which need to be fully verified. At present, the results only show that lncRNA MIR4435-2HG may be upstream of the TAZ gene and that miR-125a-5p may be downstream of the TAZ gene. At present, inhibition and promotion remain at the level of the gene and miRNA, which is not convincing. We should find the inhibitor or activator of the compound for validation tests.

In summary, lncRNA MIR4435-2HG functions as a ceRNA against miR-125a-5p and promotes neuroglioma development by upregulating TAZ. LncRNA MIR4435-2HG and miR-125a-5p are likely the upstream and downstream influencing factors of TAZ. This may be the mechanism by which TAZ promotes tumor growth and development. At present, research on the noncoding region long-chain RNA is a hot topic. LncRNA MIR4435-2HG is likely another target for the treatment of gliomas. Through studying lncRNA MIR4435-2HG and TAZ gene, a specific drug for gliomas will likely be discovered.

CONFLICT OF INTEREST

The authors declare that there is no conflict of interest.

DATA AVAILABILITY STATEMENT

The data used to support the findings of this study are available from the corresponding author upon request.

ORCID

Yun Jin https://orcid.org/0000-0002-1308-689X

REFERENCES

1. Seidu RA, Wu M, Su Z, Xu H. Paradoxical role of high mobility group box 1 in glioma: a suppressor or a promoter? *Oncol Rev*. 2017;11(1):325.
2. Murakami M, Ushio Y, Morino Y, Ohta T, Matsukado Y. Immunohistochemical localization of apolipoprotein E in human glial neoplasms. *J Clin Invest*. 1988;82(1):177-188.
3. Elbediwy A, Thompson BJ. Evolution of mechanotransduction via YAP/TAZ in animal epithelia. *Curr Opin Cell Biol*. 2018;51:117-123.
4. Kofler M, Speight P, Little D, Di Ciano-Oliveira C, Szaszi K, Kapus A. Mediated nuclear import and export of TAZ and the underlying molecular requirements. *Nat Commun*. 2018;9(1):4966.
5. Debaugnies M, Sanchez-Danes A, Rorive S, et al. YAP and TAZ are essential for basal and squamous cell carcinoma initiation. *EMBO Rep*. 2018;19(7):e45809.
6. Misra JR, Irvine KD. The Hippo signaling network and its biological functions. *Annu Rev Genet*. 2018;52:65-87.
7. Ge L, Li DS, Chen F, Feng JD, Li B, Wang TJ. TAZ overexpression is associated with epithelial-mesenchymal transition in cisplatin-resistant gastric cancer cells. *Int J Oncol*. 2017;51(1):307-315.
8. Malik SA, Khan MS, Dar M, Hussain MU, Mudassar S. TAZ is an independent prognostic factor in non-small cell lung carcinoma: elucidation at protein level. *Cancer Biomark*. 2017;18(4):389-395.
9. Huang X, Tang F, Weng Z, Zhou M, Zhang Q. MiR-591 functions as tumor suppressor in breast cancer by targeting TCF4 and inhibits Hippo-YAP/TAZ signaling pathway. *Cancer Cell Int*. 2019;19:108.
10. Rivas S, Antón IM, Wandosell F. WIP-YAP/TAZ as a new pro-oncogenic pathway in glioma. *Cancers*. 2018;10(6):191.
11. Lin H, Li P, Zhang N, Cao L, Gao YF, Ping F. Long non-coding RNA MIR503HG serves as a tumor suppressor in non-small

cell lung cancer mediated by wnt1. *Eur Rev Med Pharmacol Sci*. 2019;23(24):10818-10826.
12. Yang Y, Yang L, Liu Z, Wang Y, Yang J. Long noncoding RNA NEAT 1 and its target microRNA-125a in sepsis: correlation with acute respiratory distress syndrome risk, biochemical indexes, disease severity, and 28-day mortality. *J Clin Lab Anal*. 2020;34(12):e23509.
13. Yu H, Peng S, Chen X, Han S, Luo J. Long non-coding RNA NEAT1 serves as a novel biomarker for treatment response and survival profiles via microRNA-125a in multiple myeloma. *J Clin Lab Anal*. 2020;34(9):e23399.
14. Li Z, Tan H, Zhao W, et al. Integrative analysis of DNA methylation and gene expression profiles identifies MIR4435-2HG as an oncogenic lncRNA for glioma progression. *Gene*. 2019;715:144012.
15. Di Palo A, Siniscalchi C, Mosca N, Russo A, Potenza N. Proto-oncogene Zbtb7a represses miR-125a-5p transcription in hepatocellular carcinoma cells. *Mol Biol Rep*. 2020;47(6):4875-4878.
16. Youngblood H, Cai J, Drewry MD, et al. Expression of mRNAs, miRNAs, and lncRNAs in human trabecular meshwork cells upon mechanical stretch. *Invest Ophthalmol Vis Sci*. 2020;61(5):2.
17. Komori T. The 2016 WHO classification of tumours of the central nervous system: the major points of revision. *Neurol Med Chir*. 2017;57(7):301-311.
18. Liu R, Qin XP, Zhuang Y, et al. Glioblastoma recurrence correlates with NLGN3 levels. *Cancer Med*. 2018:7(7):2848-2859.
19. Li Y, Yang F, Gao M, et al. miR-149-3p regulates the switch between adipogenic and osteogenic differentiation of BMSCs by targeting FTO. *Mol Ther Nucleic Acids*. 2019;17:590-600.
20. Tsukui H, Horie H, Koinuma K, et al. CD73 blockade enhances the local and abscopal effects of radiotherapy in a murine rectal cancer model. *BMC Cancer*. 2020;20(1):411.
21. Wu QB, Chen J, Zhu JW, et al. MicroRNA125 inhibits RKO colorectal cancer cell growth by targeting VEGF. *Int J Mol Med*. 2018;42(1):665-673.
22. Rajabizadeh G, Rajabizadeh Z, Shokouhi Moghadam S, Vafadoost Z. The relationship between dysfunctional attitudes and communication skills of women with an addicted husband on the verge of divorce. *Addict Health*. 2019;11(1):51-57.
23. Nunes BTD, de Mendonça MHR Simith DDB, et al. Development of RT-qPCR and semi-nested RT-PCR assays for molecular diagnosis of hantavirus pulmonary syndrome. *PLoS Negl Trop Dis*. 2019;13(12):e0007884.
24. Kim B. Western blot techniques. *Methods Mol Biol*. 2017;1606:133-139.
25. Che QI, Wang W, Duan P, et al. Downregulation of miR-322 promotes apoptosis of GC-2 cell by targeting Ddx3x. *Reprod Biol Endocrinol*. 2019;17(1):63.
26. Adan A, Alizada G, Kiraz Y, Baran Y, Nalbant A. Flow cytometry: basic principles and applications. *Crit Rev Biotechnol*. 2017;37(2):163-176.
27. Zhu Y, Cui J, Liu J, Hua W, Wei W, Sun G. Sp2 promotes invasion and metastasis of hepatocellular carcinoma by targeting TRIB3 protein. *Cancer Med*. 2020;9(10):3592-3603.
28. Valente C, D'Alessandro E, Iester M. Classification and statistical trend analysis in detecting glaucomatous visual field progression. *J Ophthalmol*. 2019;2019:1583260.
29. Nagaraja TN, Elmghirbi R, Brown SL, et al. Imaging acute effects of bevacizumab on tumor vascular kinetics in a preclinical orthotopic model of U251 glioma. *NMR Biomed*. 2021;34:e4516.
30. Roldán P, Najarro R, Di Somma A, et al. Malignant glioma developed on a patient under deep brain stimulation: pitfalls in management. *World Neurosurg*. 2019;129:85-89.
31. Kavouridis VK, Boaro A, Dorr J, et al. Contemporary assessment of extent of resection in molecularly defined categories of diffuse low-grade glioma: a volumetric analysis. *J Neurosurg*. 2019;133(5):1-11. doi:10.3171/2019.6.JNS19972
32. Agrahari V. The exciting potential of nanotherapy in brain-tumor targeted drug delivery approaches. *Neural Regen Res*. 2017;12(2):197-200.
33. Rose M, Duhamel M, Aboulouard S, et al. The role of a proprotein convertase inhibitor in reactivation of tumor-associated macrophages and inhibition of glioma growth. *Mol Ther Oncolytics*. 2020;17:31-46.
34. Hofmann S, Schmidt MA, Weissmann T, et al. Evidence for improved survival with bevacizumab treatment in recurrent high-grade gliomas: a retrospective study with ("pseudo-randomized") treatment allocation by the health insurance provider. *J Neurooncol*. 2020;148(2):373-379.
35. Thompson BJ. YAP/TAZ: drivers of tumor growth, metastasis, and resistance to therapy. *BioEssays*. 2020;42(5):e1900162.
36. Escoll M, Lastra D, Pajares M, et al. Transcription factor NRF2 uses the Hippo pathway effector TAZ to induce tumorigenesis in glioblastomas. *Redox Biol*. 2020;30:101425.
37. Zhang L, Cheng F, Wei Y, et al. Inhibition of TAZ contributes radiation-induced senescence and growth arrest in glioma cells. *Oncogene*. 2019;38(15):2788-2799.
38. Tian T, Li A, Lu H, Luo R, Zhang M, Li Z. TAZ promotes temozolomide resistance by upregulating MCL-1 in human glioma cells. *Biochem Biophys Res Commun*. 2015;463(4):638-643.
39. Li PD, Wang XJ, Shan Q, Wu YH, Wang Z. Evaluation of TAZ expression and its effect on tumor invasion and metastasis in human glioma. *Asian Pac J Trop Med*. 2014;7(10):757-760.
40. Bhat KPL, Salazar KL, Balasubramaniyan V, et al. The transcriptional coactivator TAZ regulates mesenchymal differentiation in malignant glioma. *Genes Dev*. 2011;25(24):2594-2609.

How to cite this article: Shen W, Zhang J, Pan Y, Jin Y. LncRNA MIR4435-2HG functions as a ceRNA against miR-125a-5p and promotes neuroglioma development by upregulating TAZ. *J Clin Lab Anal*. 2021;35:e24066. https://doi.org/10.1002/jcla.24066